

Pockmarks on either side of the Strait of Gibraltar: formation from overpressured shallow contourite gas reservoirs and internal wave action during the last glacial sea-level lowstand?

Ricardo León · Luis Somoza · Teresa Medialdea ·
Francisco Javier González ·
Carmen Julia Gimenez-Moreno · Raúl Pérez-López

Received: 12 May 2013 / Accepted: 25 January 2014 / Published online: 20 March 2014
© Springer-Verlag Berlin Heidelberg 2014

Abstract Integrating novel and published swath bathymetry (3,980 km²), as well as chirp and high-resolution 2D seismic reflection profiles (2,190 km), this study presents the mapping of 436 pockmarks at water depths varying widely between 370 and 1,020 m on either side of the Strait of Gibraltar. On the Atlantic side in the south-eastern Gulf of Cádiz near the Camarinal Sill, 198 newly discovered pockmarks occur in three well localized and separated fields: on the upper slope ($n=14$), in the main channel of the Mediterranean outflow water (MOW, $n=160$), and on the huge contourite levee of the MOW main channel ($n=24$) near the well-known TASYO field. These pockmarks vary in diameter from 60 to 919 m, and are sub-circular to irregularly elongated or lobate in shape. Their slope angles on average range from 3° to 25°. On the Mediterranean side of the strait on the Ceuta Drift of the western Alborán Basin, where pockmarks were already known to occur, 238 pockmarks were identified and grouped into three interconnected fields, i.e. a northern ($n=34$), a central ($n=61$) and a southern field ($n=143$). In the latter two fields the pockmarks are mainly sub-circular, ranging from 130 to 400 m in diameter with slope angles averaging 1.5° to 15°. In the northern sector, by contrast, they are elongated up to 1,430 m, probably reflecting MOW activity. Based on seismo-stratigraphic interpretation, it is inferred that most pockmarks formed during and shortly after the last glacial sea-level lowstand, as they are related to the final erosional discontinuity sealed by Holocene transgressive deposits. Combining these findings with other existing knowledge, it

is proposed that pockmark formation on either side of the Strait of Gibraltar resulted from gas and/or sediment pore-water venting from overpressured shallow gas reservoirs entrapped in coarse-grained contourites of levee deposits and Pleistocene palaeochannel infillings. Venting was either triggered or promoted by hydraulic pumping associated with topographically forced internal waves. This mechanism is analogous to the long-known effect of tidal pumping on the dynamics of unit pockmarks observed along the Norwegian continental margin.

Introduction

Pockmarks, mud volcanoes, brine lakes, hydrocarbon-derived authigenic carbonate (HDAC) deposits and carbonate-mud mounds are seabed expressions of active fluid and/or gas flow associated with intensive geological, geochemical, thermal and biological activities (e.g. Dando and Hovland 1992; Judd and Hovland 2007; Foucher et al. 2009). Since the turn of the century, the scientific community has focused increasingly on the widespread occurrence of seabed fluid flow and its importance in relation to global carbon fluxes, petroleum geology exploration, climate change, tectonic activity, geomicrobiology, geohazards and as a potential future energy resource (e.g. Paull and Dillon 2001; Judd and Hovland 2007).

Pockmarks are circular to elliptically shaped craters commonly formed by localized expulsion of gas and/or liquids from an overpressured source at depth through overlying low-permeability cover sediments (Hovland and Judd 1988; Kelley et al. 1994). They occur either as isolated features or in clusters (Judd and Hovland 2007), and vary widely in size from so-called unit pockmarks of <5 m diameter, through so-

Responsible editors: B.W. Flemming and M.T. Delafontaine

R. León (✉) · L. Somoza · T. Medialdea · F. J. González ·
C. J. Gimenez-Moreno · R. Pérez-López
Marine Geology Division, Geological Survey of Spain IGME,
Rios Rosas 23, 28003 Madrid, Spain
e-mail: r.leon@igme.es

called normal pockmarks reaching 200 m in diameter, to yet larger-scaled giant and (rare) mega-pockmarks (e.g. Ondréas et al. 2005; Sahling et al. 2008; Brothers et al. 2011).

The formation of normal pockmarks has been inferred to be facilitated by tectonic control related to structural bedrock surfaces (e.g. Shaw et al. 1997), salt diapirs (e.g. Schmuck and Paull 1993; Taylor et al. 2000), or faults and faulted anticlines (e.g. Bøe et al. 1998; Eichhubl et al. 2000; Gay et al. 2004; León et al. 2010) which act as pathways for fluid migration. Furthermore, gas hydrate dissociation can be crucial to pockmark generation on continental slopes (e.g. Vogt et al. 1999; Wood et al. 2002; Hovland et al. 2005). Normal pockmarks are associated with continuous or sporadic focused gas and/or pore-water seepages, whereby pockets of overpressured gas and pore water erupt through the seafloor (Cathles et al. 2010). The freshly created pockmarks are subsequently maintained by weaker but lengthier, repeated seepages plausibly induced by tidal activity and/or, as more recently demonstrated, localized current upwelling (e.g. Hammer et al. 2009; Pau et al. 2014). In the case of the smaller “unit” pockmarks, their generation and maintenance is driven by tidal pumping of an underground “piston” of a local accumulation of subsurface free gas (Hovland and Judd 1988; Hovland et al. 1999, 2010). Occurrence of normal and unit pockmarks may thus reflect a “hydraulically active seafloor” (Hovland et al. 2012a, b).

Based on existing knowledge (cf. Somoza et al. 2012) and a new extensive acoustic and seismic dataset collected in 2010, the present article explores the distribution of pockmarks on either side of the Strait of Gibraltar with the aim of conducting a first comparative morpho-structural analysis of pockmarks in this region. Moreover, as the study area is characterised by strong tide-induced currents and the occurrence of internal waves (Bruno et al. 2002), a hydraulic pumping mechanism for pockmark formation similar to that proposed by Hovland et al. (2010) for the Norwegian margin is envisaged.

Oceanographic and geological setting

The Strait of Gibraltar separates two geological provinces, the Gulf of Cádiz (GoC) and the Alborán Basin, by the Gibraltar Arc orogenic belt which links the Betic mountains (southern Iberia) and the Rif mountains (northern Africa; Fig. 1). The Alborán Basin fill is composed of Early Miocene to Quaternary marine deposits, and its western part (western Alborán Basin, WAB) is affected by mud diapirism (overpressured Early Miocene shales) triggered by tectonic compression and sediment overburden since the Middle Miocene (Comas et al. 1992; Vázquez and Vegas 1996; Pérez-Belzuz et al. 1997). In the GoC, two tectonic provinces surround the internal zones of the Gibraltar Arc orogenic belt: the Flysch Complex of the Campo de Gibraltar and the Betic

External Zones, both extensively outcropping on the southwestern Iberian continental shelf and upper slope (Maldonado et al. 1999; Esteras et al. 2000; Medialdea et al. 2004). Two types of diapirism have been recognized in this area: (1) salt diapirism related to Mesozoic evaporites and (2) marly diapirism related to the Gulf of Cádiz unit (Medialdea et al. 2004; Fernández-Puga et al. 2007).

Associated with this diapirism, intense fluid flow activity has been observed both in the GoC (Ivanov et al. 2000; Somoza et al. 2000, 2003; Gardner 2001) and in the WAB (Pérez-Belzuz et al. 1997; Talukder et al. 2003; Blinova et al. 2011). In the study area, previous investigations mainly focused on seabed fluid flow structures such as mud volcanoes (Fig. 2) and HDAC fields, both in the GoC (Ivanov et al. 2000, 2001; Somoza et al. 2000, 2003; Díaz-del-Río et al. 2003; León et al. 2006, 2012; Medialdea et al. 2009; Magalhães et al. 2012) and the WAB (Kenyon et al. 2000, 2003, 2006; Comas et al. 2003; Talukder et al. 2003; Ivanov et al. 2010; Blinova et al. 2011; Somoza et al. 2012). The pockmarks and crater-like depressions themselves, however, received little attention in these earlier studies. In the GoC, they have only been reported west of the study area at water depths of 850–1,450 m (Baraza and Ercilla 1996; León et al. 2006, 2010). In the WAB, Blinova et al. (2011) reported localized pockmarks and so-called crown-foot pockmarks close to volcanic edifices. Somoza et al. (2012) for the first time identified pockmarks and stacked buried palaeo-pockmarks in the Ceuta Drift. These occur in several fields in 400–900 m water depth, and appear rooted in shallow subsurface reservoirs which have been active since at least the mid-Pleistocene (Ivanov et al. 2010; Blinova et al. 2011; Somoza et al. 2012). The geochemistry of hydrocarbons and biomineralizations suggest that, in the GoC, these are thermogenic and biogenic in origin (Ivanov et al. 2000; Díaz-del-Río et al. 2003; Stadnitskaia et al. 2006; González et al. 2012), whereas in the WAB a dominant deep-seated thermogenic source has been identified (Poludetkina and Kozlova 2003; Blinova et al. 2011).

The Strait of Gibraltar (81–2,000 m depth) constitutes the gateway connecting Mediterranean and Atlantic water masses (Fig. 1; for recent overview of Iberian Peninsula water mass dynamics and associated sedimentary processes, see Hernández-Molina et al. 2011). The circulation pattern is characterised by eastward-flowing Atlantic water (AW) in the upper layer entering the Mediterranean Sea, and warm, dense and highly saline westward-flowing Mediterranean outflow water (MOW) in the bottom layer entering the Atlantic (Ambar et al. 2002). The AW is composed largely of North Atlantic Surface Water (NASW); the MOW consists of Levantine Intermediate Water (LIW), which flows westwards at depths of 200–600 m, and Western Mediterranean Deep Water (WMDW) which occurs at greater depths mainly along the Moroccan margin (Millot 1999; Fig. 1). The nascent MOW intrudes the subsurface layers of the GoC at more than

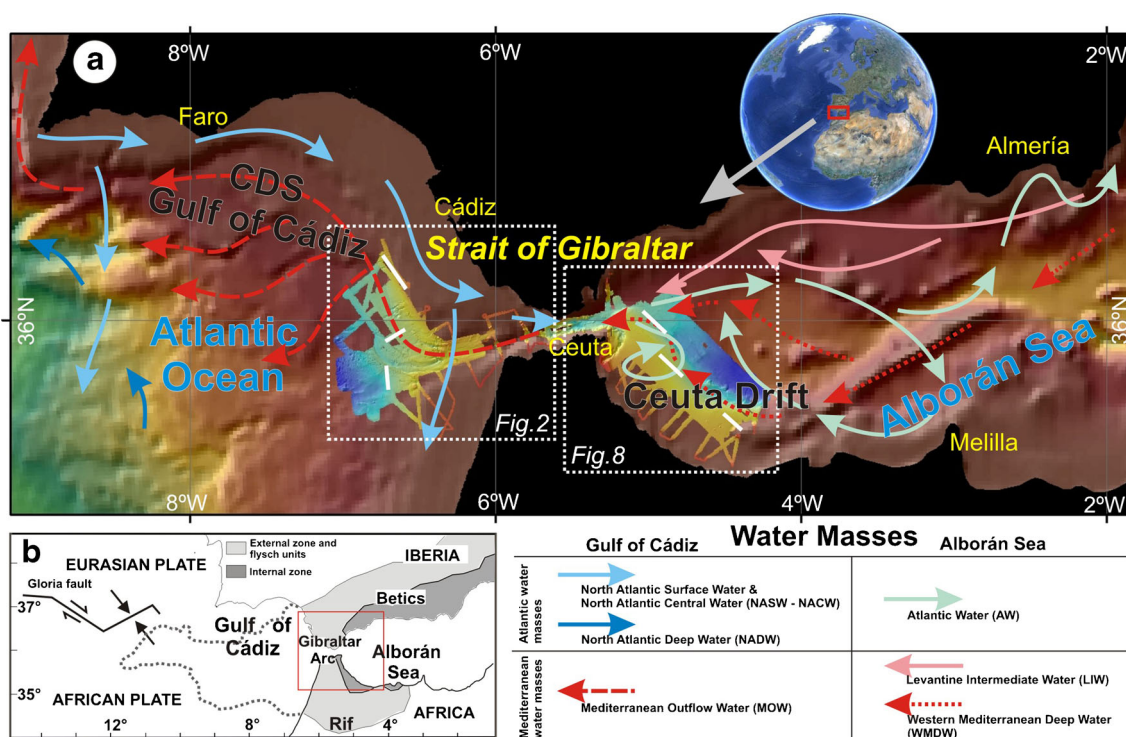


Fig. 1 a Regional water mass circulation along the southern Iberian margin (modified from Hernández-Molina et al. 2006, 2008), superimposed on the bathymetry. Red–blue shadings areas of multibeam and seismic data acquisition, white lines tracks of cruise Contouriber-1. b Geological framework of the study areas in the Gulf of Cádiz (eastern sector) and the Alborán Sea (Ceuta Drift)

200 cm s⁻¹ (Ambar and Howe 1979), driven by its higher density in comparison to the lower-density North Atlantic Central Water (NACW; Gasser et al. 2011). Thereafter, the MOW is deflected north-westwards into the GoC from where it progressively descends obliquely to the continental slope, flowing from the SE to the NW at 40–80 cm s⁻¹ along channels and moats until it loses contact with the seafloor at 1,000–1,400 m water depth above the North Atlantic Deep Water (NADW; Ambar and Howe 1979; Hernández-Molina et al. 2003, 2012).

In the Strait of Gibraltar, large (more than 100-m-high) internal waves have been observed (Nakamura and Awaji 2001; Bruno et al. 2002), being probably generated by the interaction between barotropic tidal flow and the topography of the main sill (Camarinal Sill) and the stratified water column (Vázquez et al. 2008). Upon entering the Mediterranean, the internal waves significantly affect the hydrography of the Alborán Sea (Vázquez et al. 2008).

From the Pliocene to the Present, the interaction of Mediterranean water masses with adjacent continental slopes has resulted in the formation of contourite depositional systems (CDSs) on both sides of the strait (Fig. 1). In the WAB, the Ceuta CDS (200–700 m water depth) is an elongated plastered drift up to 700 ms TWT (two-way travel time) thick, 100 km long and 28 km wide. It is composed mainly of mud with intercalations of a thick sandy mud layer deposited during the last glacial sea-level lowstand and a thinner silty clay layer emplaced during the ensuing sea-level highstand

(Ercilla et al. 2002). Brackenridge et al. (2011) have integrated the Ceuta CDS within a revised deep-water sequence stratigraphic framework.

On the Atlantic side, the study area only covers the part of the CDS in the GoC (at 300–1,200 m water depth; Faugères et al. 1984) known as the proximal scour and sand-ribbon sector (Habgood et al. 2003; Hernández-Molina et al. 2003). This sector is dominated by a wide channel (the so-called main channel; Hernández-Molina et al. 2012) with scour alignments, abrasion surfaces, dunes and sand-ribbon fields. A huge contourite levee, generated by MOW overflow, is located south-westwards of the main channel and is composed of sand/mud sedimentary lobes and sand/mud wave fields with slides and furrows (Hernández-Molina et al. 2006; Hanquiez et al. 2007). To the north of the main channel, a thick (~815 m) sandy sheeted drift composed of muddy, silty, and sandy sediments is present, the sand layers averaging 12–15 m in thickness (Buitrago et al. 2001).

(Ercilla et al. 2002). Brackenridge et al. (2011) have integrated the Ceuta CDS within a revised deep-water sequence stratigraphic framework.

Materials and methods

The dataset presented in this paper was acquired in 2010 during the Contouriber-1 cruise onboard the R/V *Sarmiento de Gamboa* (Fig. 1). High-resolution seismic reflection data were obtained using an array of three air guns (140+300+90 cubic inches) and a 150 m streamer composed of three

sections of 40 hydrophones each. The shot interval was 6 s and the recording length 5 s. Data processing was performed with the Hot Shots™ software.

Ultrahigh-resolution chirp profiles were acquired simultaneously by means of a parametric echosounder (ATLAS Parasound P35) operating at a primary high frequency of 18 kHz and a secondary lower frequency of 3.5–4 kHz. Bathymetric data were acquired by means of an ATLAS Hydrosweep DS multibeam echosounder (MBES) system operated at 14.5–16 kHz with 140 beams at pulse lengths of 0.17–25 ms and a vertical resolution of 0.5 m. Bathymetric and backscatter data were processed using the CARIS™ software. Density maps were developed using the “kernel density tool” of ArcGIS software of ESRI. In addition, periodic CTD measurements and SIPPICAN XBT casts were made to determine the vertical temperature characteristics of the water column (precision ± 0.15 °C).

Statistical morphological analyses (cf. Pérez-López et al. 2011) included the establishment of a size-frequency distribution of pockmarks (expressed in m^2) for each field of the study area. The exponential trend (Eq. 1) derived from the size-frequency distribution suggests that the natural processes responsible for the pockmark size (shape) distribution obey the following relationship:

$$N(A) = \alpha \cdot \exp^{\beta \cdot A} \quad (1)$$

where $N(A)$ is the number of pockmarks with area greater than or equal to A , and α and β are constants relating to the least squares method for logarithmic fitting.

Results

Maps showing the distribution of pockmarks on either side of the Strait of Gibraltar, i.e. in the eastern GoC and the WAB, are presented here for the first time. Based on chirp seismic profiles and multibeam bathymetry, a total of 436 pockmarks were mapped, comprising 198 newly identified ones from the GoC and 238 pockmarks previously reported by Somoza et al. (2012) from the WAB. Based on their morphology, distribution, hosting sediments and hydrodynamic environments, the pockmarks were grouped into distinct fields.

Gulf of Cádiz

Three main pockmark fields were identified in the GoC study area at water depths ranging strongly from 350–1,020 m. These fields are referred to as the upper slope, the main channel, and the TASYO fields (Fig. 2, Table 1).

Upper slope field

The upper slope pockmark field is located on the upper slope of the Iberian continental margin at water depths of 350–600 m, this being the shallowest yet observed on the Atlantic side of the Strait of Gibraltar (Fig. 2). This paper reports first MBES bathymetric images from this field (Figs. 2 and 3), supported by ultrahigh-resolution seismic profiles (Fig. 4). The MBES mosaic partially covers the field over a distance of 10 km, revealing a low pockmark density ranging in cumulative area from 400–8,350 $m^2 km^{-2}$ (Fig. 3). Less than 0.9 km^2 of the field is affected by pockmarks visible on the seabed. MBES images show a cluster of gullies running downslope in a NE–SW direction between 350 and 450 m water depths, fading out at the northern boundary of the MOW channel (Fig. 4). Circular pockmarks between gullies can also be seen on the images.

The pockmarks in this field occur as isolated oval to near-circular and up to 16-m-deep seabed depressions, ranging from 70–760 m in maximum diameter. They are grouped around modal size classes of 90 and 440 m. The statistical morphological analysis shows each of the two size classes to follow a different logarithmic law, the small size class having a β value of -2 (US 1, Fig. 3a), the large size class of -1 (US 2, Fig. 3a). The smaller pockmarks (90 m modal class) are located between the gullies (iP, Fig. 4a), whereas the larger ones (440 m modal class) are located within the gullies (Pg, Fig. 4a). These isolated pockmarks have a high eccentricity index (ratio between short/long axes) grouped around a mode of 0.75 relating to sub-circular geometries. The azimuths of the long axes show two modes: a clear one at $45^\circ N$ for the large sizes, and $\sim 160^\circ N$ for the small ones (Fig. 3). The pockmarks have a flat floor with flanks sloping at $3\text{--}7^\circ$, maximum values of 10° being restricted to the larger sizes (pockmarks in gullies). In addition, the large sub-circular pockmarks seem to merge into northeast–southwest elongated seabed depressions in the downslope segments of the gullies (Fig. 4), as reported from similar settings worldwide (e.g. eastern Black Sea, Çifçi et al. 2003). As the pockmarks within the gullies were identified from chirp seismic profiles (Fig. 5), it was not immediately clear whether the apparent seabed craters represented semi-circular gas escape structures or merely erosional channels within gullies crossed by the seismic lines. Taking into account the characteristics of these structures, this aspect is clarified below.

On chirp profiles, the circular pockmarks of the upper slope field display small funnel-shaped seabed depressions about 12 ms TWT in depth (i.e. about 10 m at an average velocity of $1,750 m s^{-1}$) and rooted in slightly transparent layers (Fig. 5). In most cases the depressions are draped by 2–3 ms TWT ($1.75\text{--}2.5 m$ at $1,750 m s^{-1}$) parallel reflectors which partially fill the funnels (Fig. 5b). A high negative amplitude anomaly is sometimes observed at the apexes of the funnel-shaped depressions.

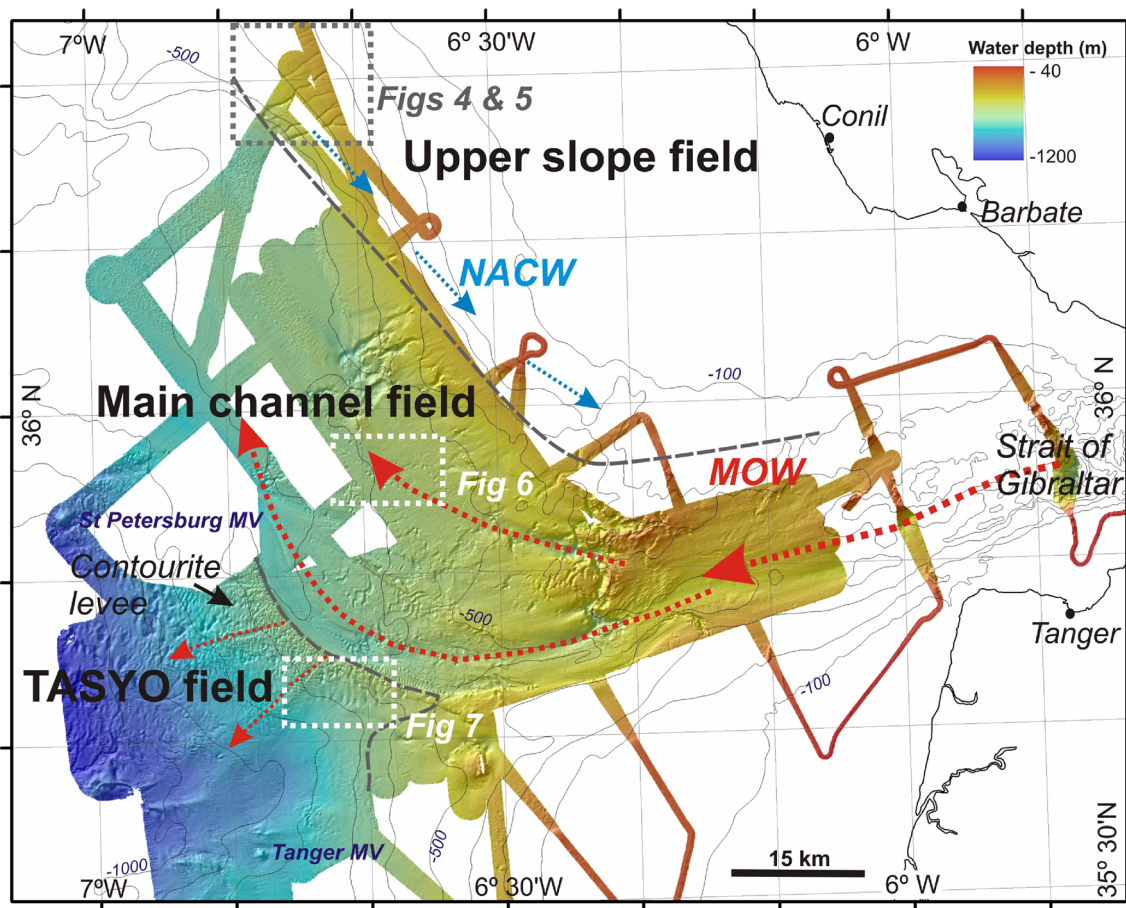


Fig. 2 Multibeam bathymetry of the eastern Gulf of Cádiz. *Grey dashed lines* Locations of new pockmark fields, *black dots* pockmarks

Chirp profiles crossing the gullies and isolated pockmarks (Fig. 5b) show the following sequence of reflectors (Fig. 5a): (1) a concave reflector expressing a subdued topographic seafloor, overlain by a N–S prograding wedge filling the depression, (2) funnel-shaped acoustically transparent structures and (3) a drape package consisting of a sequence of onlapping parallel reflectors filling the funnel structures. Beneath the depressions, slightly bent blanking columns associated with normal faults probably represent the pathways of upward gas migration (Fig. 5a). The fact that the vertical acoustic blanking columns fade out below the concave reflector (cf. point 1 above) implies that fluid migrates laterally (sideways) below this reflector due to the presence of high-permeability sediments (yellow dotted reflectors in Fig. 5).

Main channel field

In all, 160 pockmarks were identified and mapped in the main channel of the Mediterranean outflow in the GoC west of the Strait of Gibraltar (Figs. 2, 6) at water depths of 450–700 m. Pockmarks are mainly located between 6°20' W and 6°50' W, where the MOW flow deflects

towards the northeast (Fig. 2). About 7 km² of seafloor is affected by pockmarks in this area, with densities (cumulative areas) of 2,500–26,700 m² km⁻² (Table 1).

MBES bathymetric images show sub-circular and elongated pockmarks aligned with the axis of the channel (Fig. 6). The statistical morphological analysis again reveals two size classes each with a different logarithmic trend, the small size class now having a β value of -3 (MC 1, Fig. 3b), the large one a β of -1 (MC 2, Fig. 3b). The smaller size class comprises sub-circular depressions 60–150 m in diameter (U-P in Fig. 6a) with an eccentricity index of ~ 0.8 and flanks sloping at 4–7°. These pockmarks are commonly clustered in strings of usually 8–10 aligned along the main flow path of the MOW (Fig. 6a).

In the larger size class, pockmarks are sub-circular and 250–500 m in diameter (eP, Fig. 6a), sometimes merging to form elliptical or irregular depressions up to 1 km long. They are 5–25 m deep and their flanks have steep slopes averaging at 10–15°, with maximum slopes reaching 19°. The highly elliptical geometries reach eccentricity indices around 0.4, the azimuths of the depressions being oriented 56°N and 135°N. The saw-shaped morphology of the channel in this sector

Table 1 Main features and morphological parameters of the pockmark fields in the eastern Gulf of Cádiz area

Field	Eastern Gulf of Cádiz area					
		Upper slope	Main channel	TASYO		
Water depth (m)		350–600	450–700	450–1,020		
Number		14	160	24		
Area affected (km ²)		0.9	7	2.7		
Density (m ² km ⁻²)		400–8,350	2,500–26,700	1,500–14,000		
Shape		Single, sub-circular, symmetrical, V-shaped	Sub-circular to elongated, cone-shaped, chains	Lobate, elongated, freak sedimentary waves		
Depth (m)		16–25	5–25	40–60		
Long axis (m)	Range	70–764	60–909	126–919		
	Mode	90; 440	203	320; 720		
Short axis (m)	Range	182–491	53–595	111–487		
	Mode	91; 250	95	250		
Eccentricity (short axis/long axis)	Range	0.44–0.99	0.39–1	0.2–0.96		
	Mode	0.7	0.45; 0.8	0.65		
Azimuth (°)	Range	45–180	0–180	1–177		
	Mode	45; 160	56; 135	0; 45		
Slope (°)	Mean	3–4	10–15	15–25		
	Max.	10	19	35		
Seismics		Funnel-shaped depressions, thin sedimentary drape	Cone-shaped	Irregular depressions over transparent columnar disturbances		
Statistical analyses						
Sub-field		US 1	US 2	MC 1	MC 2	
Area range (km ²)		4–20	20–280	3–70	70–391	11–356
<i>A</i>		14	10	173	60	28
<i>β</i> exp-5		-2	-1	-3	-1	-1
Correlation coefficient		0.85	0.94	0.99	0.95	0.99

suggests that it was formed by retrogradational erosion involving strings of pockmarks (Fig. 6a).

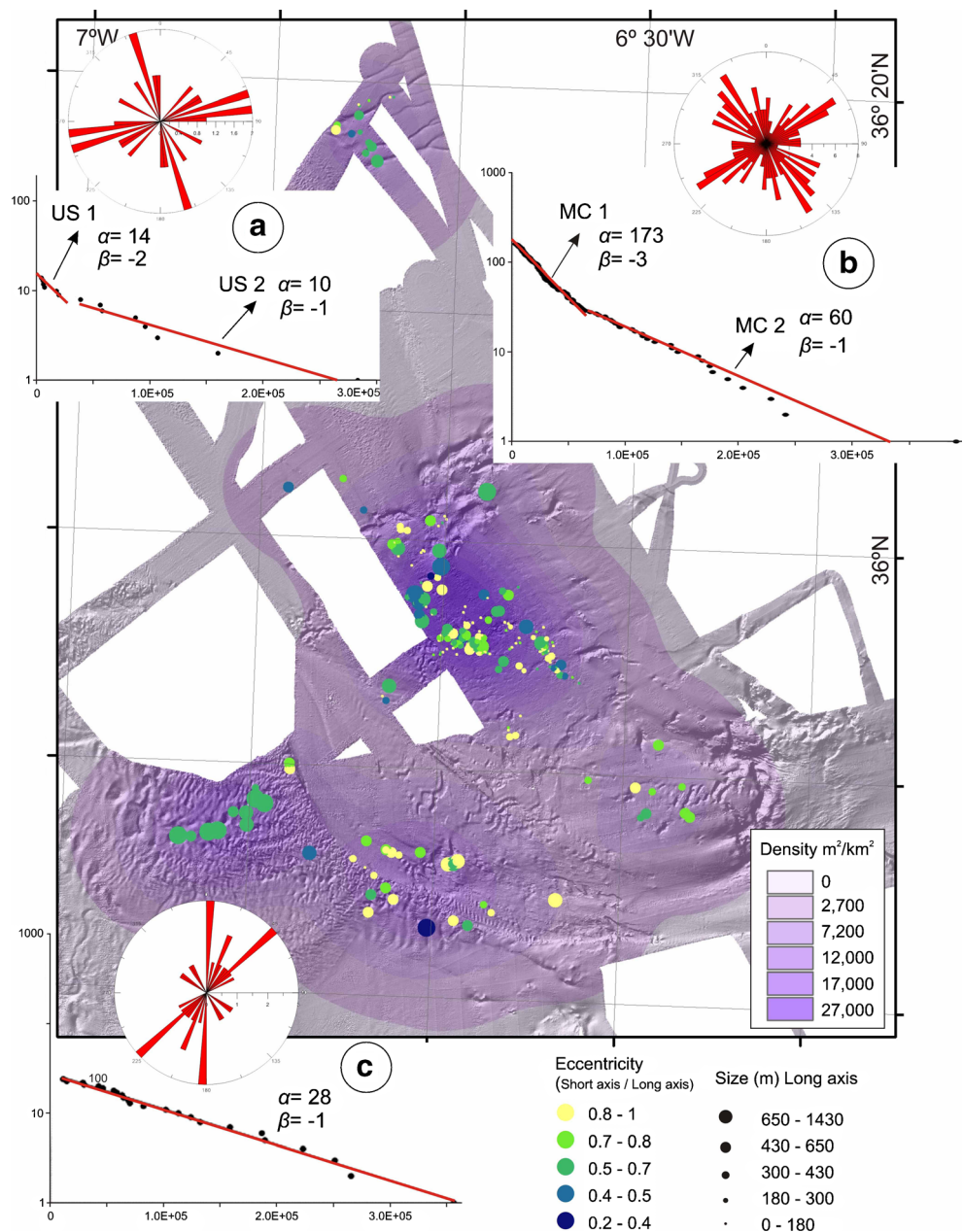
In the high-resolution seismic profiles of the MOW main channel pockmark field (Fig. 6), vertical acoustic chimneys with high-amplitude anomalies are connected to deep-rooted diapirs located below the field. These acoustic chimneys are interpreted as representing fluid migration conduits produced by the upward movement of Miocene marly diapirs of the GoC (cf. Maldonado et al. 1999). The seismic images show that the acoustic chimneys do not reach the seafloor. However, channel-shaped bodies with mounded and complex sedimentary fills appear at the top of the chimneys below the pockmark field (Fig. 6). These sediment bodies are interpreted to represent palaeochannels of the MOW undercurrent, probably generated by intensification of MOW flow during the mid-Pleistocene revolution, as suggested by correlations with the results of the IODP expedition 339 in the GoC (cf. Stow et al. 2011). It is inferred that coarse-grained sands of buried contourite palaeochannels form shallow subsurface reservoirs (at depths of 1–0.5 s TWT) which feed the pockmarks.

TASYO field

The TASYO field was first described by Somoza et al. (2003). It shows a characteristic “smallpox”-like seabed morphology with abundant expressions of hydrocarbon seeps in the form of mud volcanoes (e.g. Tasyo, Hespérides, Faro, Aveiro, St. Petersburg). This field is located in the area of overflow of the MOW undercurrent at water depths between 450–1,020 m (Fig. 7a). The field is thus bound upslope by the contourite levee of the main MOW channel and downslope by the termination of several furrows, such as the Gil Eanes (e.g. Hernández-Molina et al. 2003; Mulder et al. 2003). An influence of episodic warming of Mediterranean waters on gas hydrate dissociation has been proposed as an explanation for the characteristic morphology of this area (Gardner 2001).

In the present paper, only those pockmarks were mapped which relate to the huge contourite levee (sand bank, Figs. 2, 7a) generated by MOW overflow processes. The pockmarks lack a clear seafloor expression because they are masked by the occurrence of sandy contourite deposits and sediment waves. However, they can be identified on MBES images by

Fig. 3 Spatial distribution of pockmarks in the eastern field of the GoC. Long axes are symbolized by dots of different size and colour in accordance with their eccentricity, superimposed on a shaded pockmark population density plot. Cumulative size-frequency plots and rose diagrams showing the azimuths of pockmark long axes: **a** the upper slope field, **b** the main channel field, and **c** the TASYO field. Size-frequency plots: *x-axis* basal area in m², *y-axis* number of pockmarks with an area greater than or equal to *A*; α and β are constants (cf. Eq. 1) of the least squares method for logarithmic fitting (see [Materials and methods](#) for further explanation)



irregular depressions and steep slopes within the sediment wave field (Fig. 7a). Based on these criteria, 24 pockmarks were mapped along the contourite levee of the MOW channel. They have diameters of 125–920 m and very steep flanks of up to 30° (Fig. 7a). The pockmarks can be grouped into two size classes with diameters of about 300 and 740 m. The scattered individual pockmarks occur at densities ranging from 1,500 to 14,600 m² km⁻². The statistical morphological analysis shows only a single logarithmic trend with a β value of -1 (Fig. 3c). Their geometry is commonly smooth elongated with an eccentricity index of 0.65 and preferential long axis azimuths oriented N–S and 45°N. A point of interest regarding the sediment waves is that they have steeper flanks

(22–35°) than is normally the case. Their morphology observed on MBES images (Fig. 7a) suggests that they might be freak sediment waves of the type described by Judd and Hovland (2007) from the North Sea.

In cross section, the chirp seismic profiles show amplitude anomalies and transparent columnar disturbances beneath the pockmarks (Fig. 7b). The acoustic anomalies caused by fluid migration relate to a cluster of normal faults associated with updoming reflectors. The fact that the transparent columnar disturbances below the pockmarks are interconnected within slightly dipping transparent sedimentary units (at about 25 ms TWT depth below seabed) suggests lateral gas-rich fluid migration from shallow subsurface reservoirs. In this case,

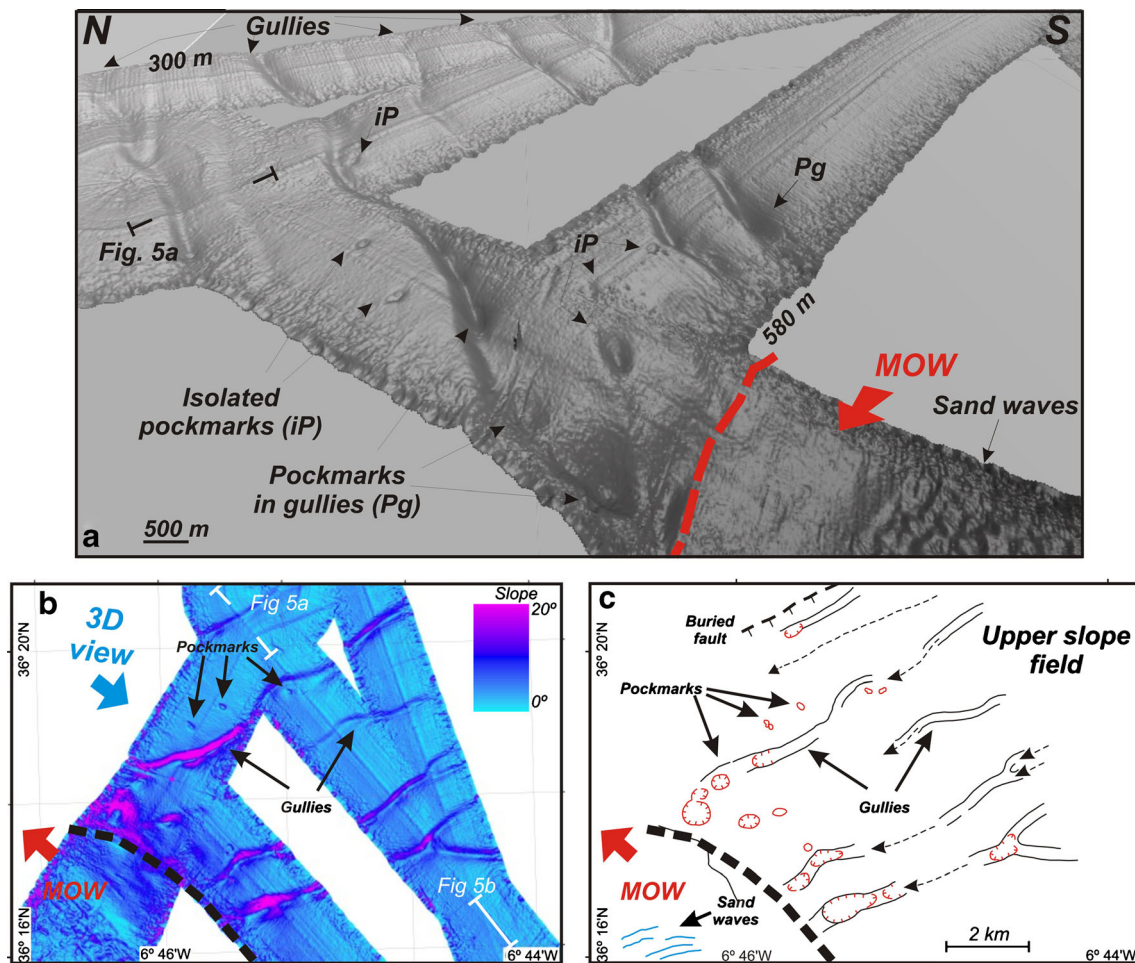


Fig. 4 Surficial expression of pockmarks in the upper slope field. **a** Detailed 3D view of isolated pockmarks and pockmarks in gullies. **b** Gradient map showing the location of subsequent figures. **c** Geomorphological scheme showing the main features and location of the pockmarks (red)

the coarse-grained palaeo-levee deposits might act as such reservoirs, as already inferred for the other pockmark fields in the GoC.

Western Alborán Basin

The pockmark fields in the WAB study area are located on the Ceuta contourite drift (Ercilla et al. 2002). Based on MBES bathymetry, 238 pockmarks have been newly mapped here at water depths of 370–880 m. The occurrence of surface and buried pockmarks in the WAB was first reported by Somoza et al. (2012). Based on the morphological analysis of the 3D multibeam dataset, this paper reports three new fields in this area: a northern, central and southern field (Fig. 8, Table 2).

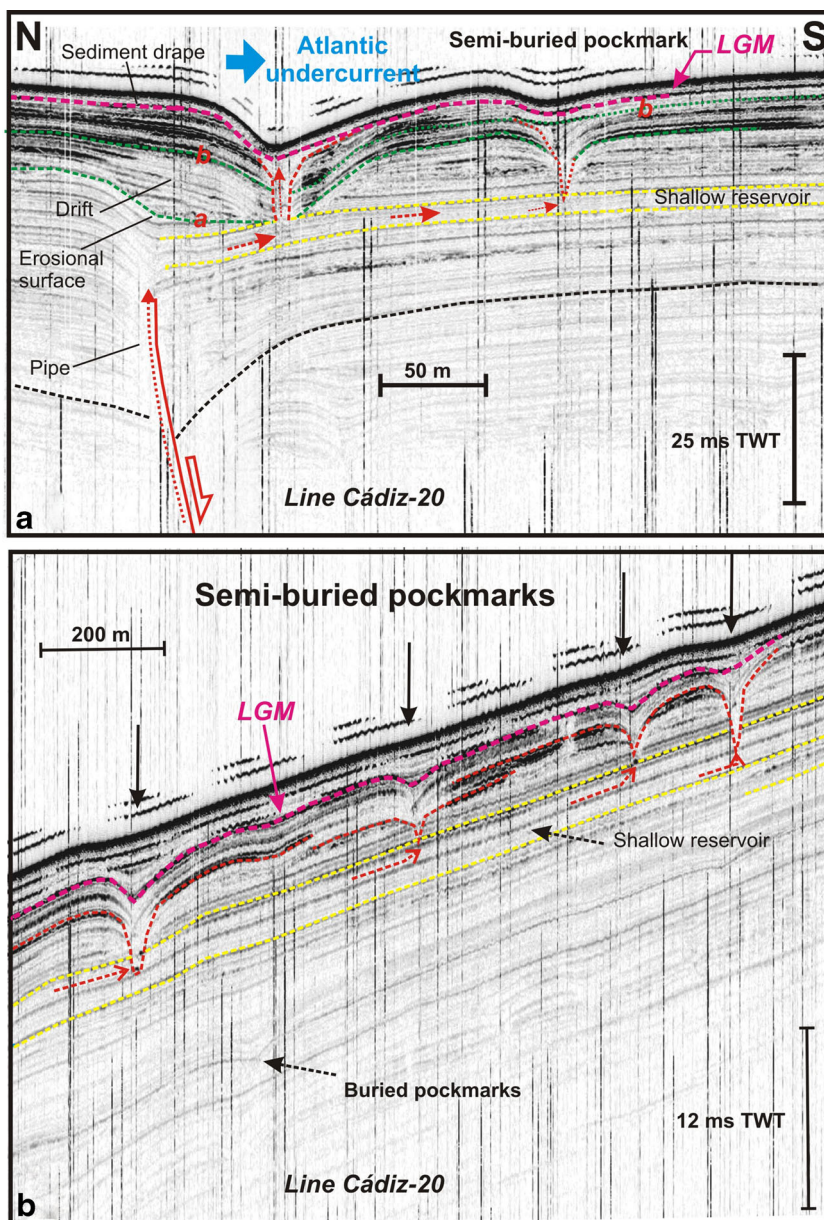
Northern field

In all, 34 pockmarks were mapped in the northern field, located near the northern limit of the Ceuta Drift at water depths of 650–880 m (Fig. 8). This field shows the highest density of pockmarks observed on the Ceuta Drift. The extent of seafloor

affected by pockmarks is about 3 km² with a crater density (cumulative area) of 8,000–24,600 m² km⁻² in the inner part of the field (Fig. 9). The pockmarks appear to be strongly affected by the Mediterranean undercurrent, as can be inferred from their morphology characterised by elongated depressions with diameters of 243–1,430 m, slope flanks of 1.35–4° and depths of 4–8 m. The statistical morphological analysis shows a single logarithmic trend with a β value of -1 (Fig. 9a). The pockmarks thus have a mostly elongated shape with eccentricity indices grouped around a modal value of 0.4, the main axes being closely aligned at about 110°N (Fig. 10b, Table 2). Locally, large lobe structures with steeply sloping flanks (8–11°) and 10 m depths may occur where neighbouring pockmarks merge (Fig. 10b).

A representative example from this field is shown in Fig. 11a. In cross section, these pockmarks display an erosional asymmetrical V-shaped depression underlain by an acoustically transparent narrow funnel which truncates adjacent strata, deforming the reflectors upwards. Localized high-amplitude anomalies are observed within the blanking funnel. The base of the transparent funnels is located on a slightly dipping transparent layer at ~25–30 ms TWT depth below

Fig. 5 Ultrahigh-resolution seismic profiles crosscutting semi-buried and buried pockmarks in the upper slope field. For location, see Fig. 4b



seabed. This transparent unit is under- and overlain by seismic units composed of well-defined reflectors. Based on these data, it is inferred that the pockmarks of the northern field have their source in this layer, interpreted to represent a shallow, high-pore pressure reservoir sealed by overlying high-reflectivity units.

Central field

The central field, at water depths of 466–597 m, has a random distribution of 61 pockmarks covering a total mapped area of 5.7 km² with densities of 11,000–24,500 m² km⁻² (Fig. 9). The statistical morphological analysis shows a single logarithmic trend with a β value of -3 (Fig. 9b). All the

pockmarks in this field have similar sub-circular morphologies (Figs. 10a, d, 11a, Table 2). Although the longer axes range from 214–613 m, their mode (400 m) and mean (398 m) are similar, the eccentricity index averaging at 0.8. The cross-sectional profiles are V-shaped with depths of 15–20 m and steeply sloping flanks of 6–15° reaching maximum values of 22° (Fig. 10a, Table 2). On the gradient map, the downslope profiles across the pockmarks are relatively smooth (“s” in Fig. 10a).

The chirp seismic profiles reveal that the V-shaped depressions are associated with transparent acoustic facies (Fig. 11a). These funnels are overlain by a thin package of parallel reflectors which are concordant with the seabed and are interpreted as the draping package. The acoustically

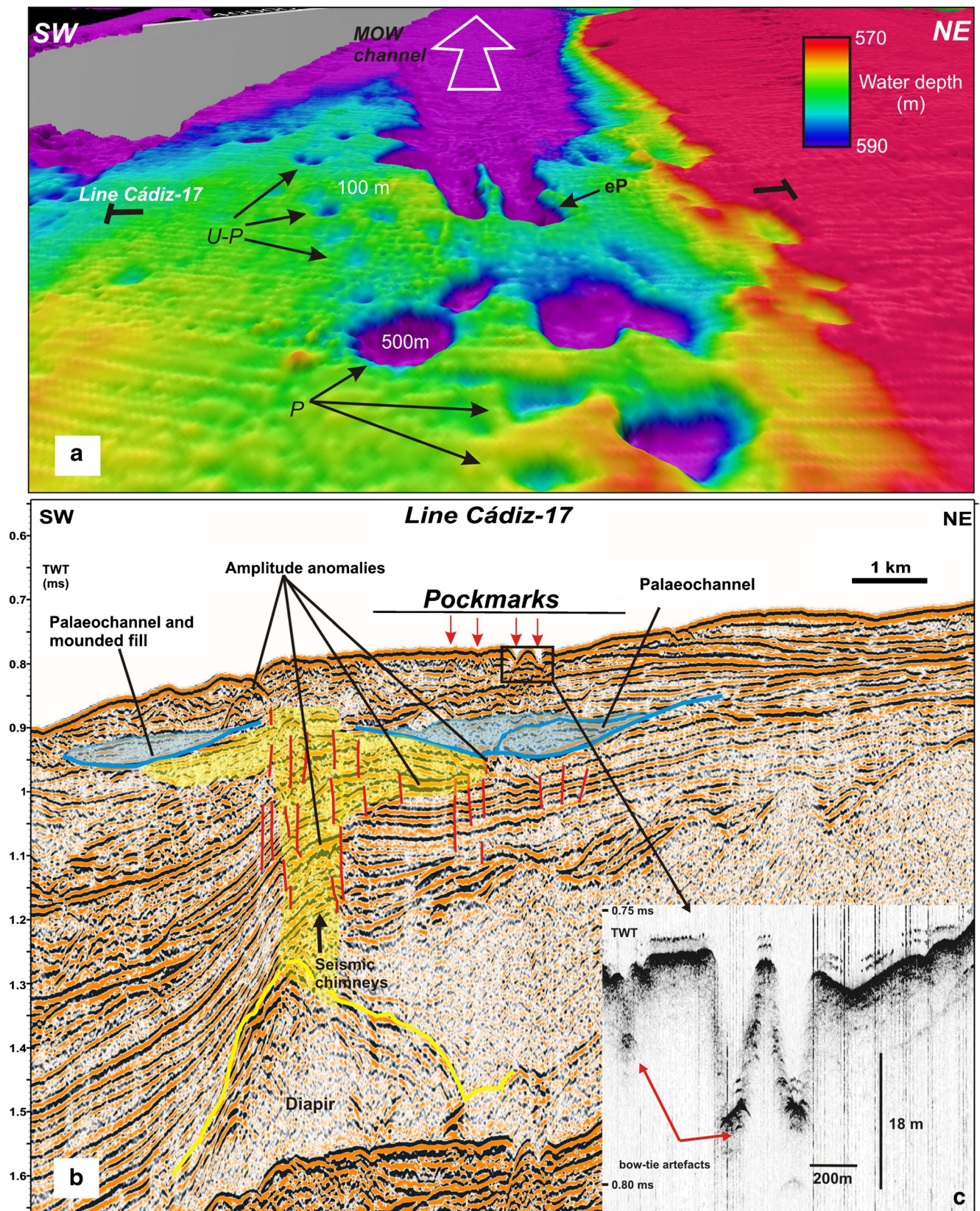


Fig. 6 **a** Shaded relief DTM of the main channel field (eastern Gulf of Cádiz) imaging different pockmarks: small circular pockmarks (*U-P*), large sub-circular ones (*P*), and merged string of pockmarks (*eP*). **b** Interpreted airgun seismic profile showing shallow gas reservoirs

associated with palaeochannels. Shallow reservoirs are fed by seepage from deeper sources related to diapirism. **c** Chirp profile for the seismic image sector marked on the inset in **b**. Note bow-tie artefacts at the base of pockmarks. For location, see Fig. 2

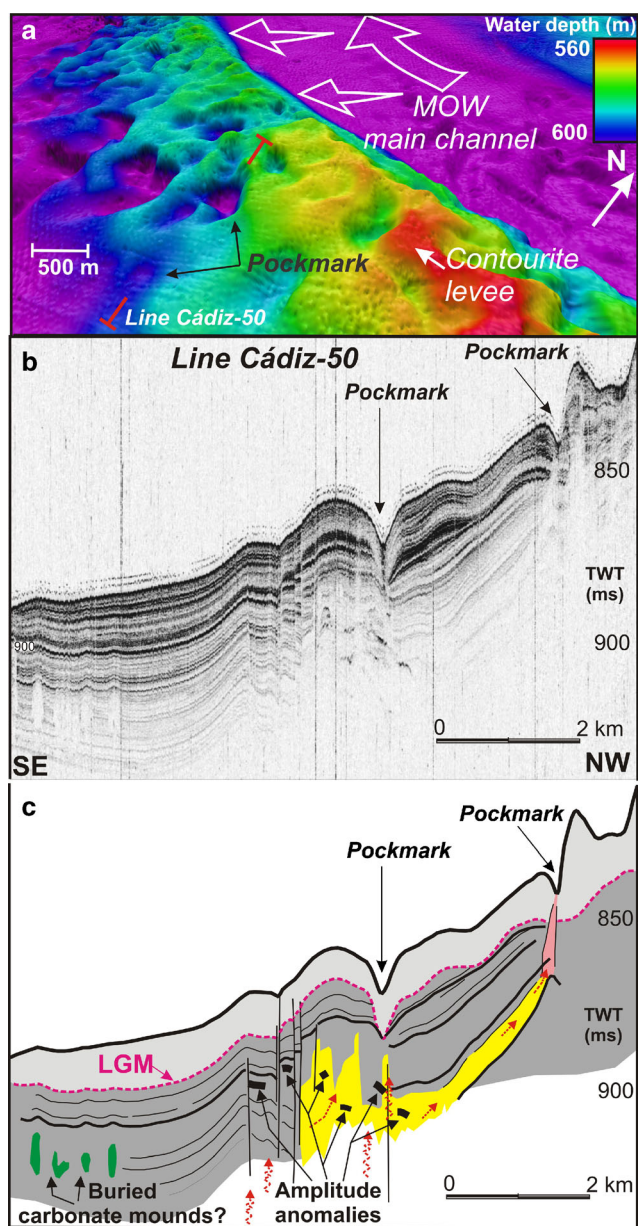


Fig. 7 TASYO field. **a** 3D shaded bathymetric view of the huge contourite levee generated by overflow processes related to the MOW, where pockmarks and sediment waves have been identified. **b, c** Non-interpreted and interpreted chirp seismic profile from a levee

transparent funnels truncate adjacent coherent reflectors with velocity pull-ups at their margins. However, the most characteristic seismic expression are triangular-shaped collapsed fragments within the funnels which are derived from the adjacent sedimentary strata (Fig. 11b). This implies that the pockmarks are not only formed by upward fluid migration but also by seabed collapse. The apexes of the transparent funnels are located on an acoustically transparent sediment layer at ~20–25 ms TWT beneath the seabed. These layers (shallow subsurface reservoirs in Fig. 11) are sealed by highly reflective units.

Southern field

A total of 143 pockmarks were mapped in the southern field covering an area of about 5 km² at water depths of 379–587 m. This is the shallowest pockmark field on the Ceuta Drift. The pockmarks are randomly distributed with a density of around 17,000 m² km⁻² in the central part of the field (Fig. 9). The statistical morphological analysis shows a single logarithmic trend with a β value of -6 (Fig. 9c). Shapes and sizes are quite similar, comprising oval and sub-circular depressions with a modal eccentricity index of 0.9. Maximum diameters range from 130–390 m. Cross-sectional profiles are U-shaped and depths are the shallowest of the study area, ranging from 0.5–1 m, associated with smoothly sloping flanks and gradients of 1.2–1.8° (Fig. 10c). A representative ultrahigh-resolution chirp profile (Fig. 11c) shows that the pockmarks have symmetrical profiles underlain by acoustically transparent columnar disturbances. They are covered by a thin layer (about 7 ms TWT) of semi-continuous and moderate- to low-amplitude reflectors concordant with the seabed representing the draping package. Feeder channels are rooted in a layer at a depth of 20–25 ms TWT beneath the seabed. The base of the transparent pipe shows pull-up effects of coherent reflectors. As in the other fields on the Ceuta Drift, the pockmarks have their source in shallow transparent sediments which evidently act as subsurface reservoirs. In contrast to those in the other fields (Fig. 11a, b) where feeder channels are relatively wide and characterised by collapse structures, the pockmarks in the southern field have very narrow feeder pipes without collapse structures (Fig. 11c).

Discussion

The WAB and GoC show different pockmark typologies based on their morphology, shape, size, density and distribution. Whereas WAB pockmarks have similar sizes and shapes and are homogeneously distributed, those of the GoC are more scattered, vary more strongly in size, are elongated in shape and aligned with the main channel of the MOW. In both cases, however, the pockmark fields are developed on contourite depositional systems generated by Mediterranean water masses, the WMDW and MOW respectively. The morphology, distribution, hosting sediments and hydrodynamic environment of the pockmark fields reveal much about their genesis and the factors controlling their development, especially the mechanisms of fluid migration from their subsurface sources to the seafloor. Of particular interest are (1) the links between source areas, buried pockmarks and the seabed, (2) the nature and role of the hydrodynamic regime to which they are exposed, and (3) differences in distribution and morphology in relation to fluid flow mechanisms and oceanographic processes on either side of the Strait of Gibraltar.

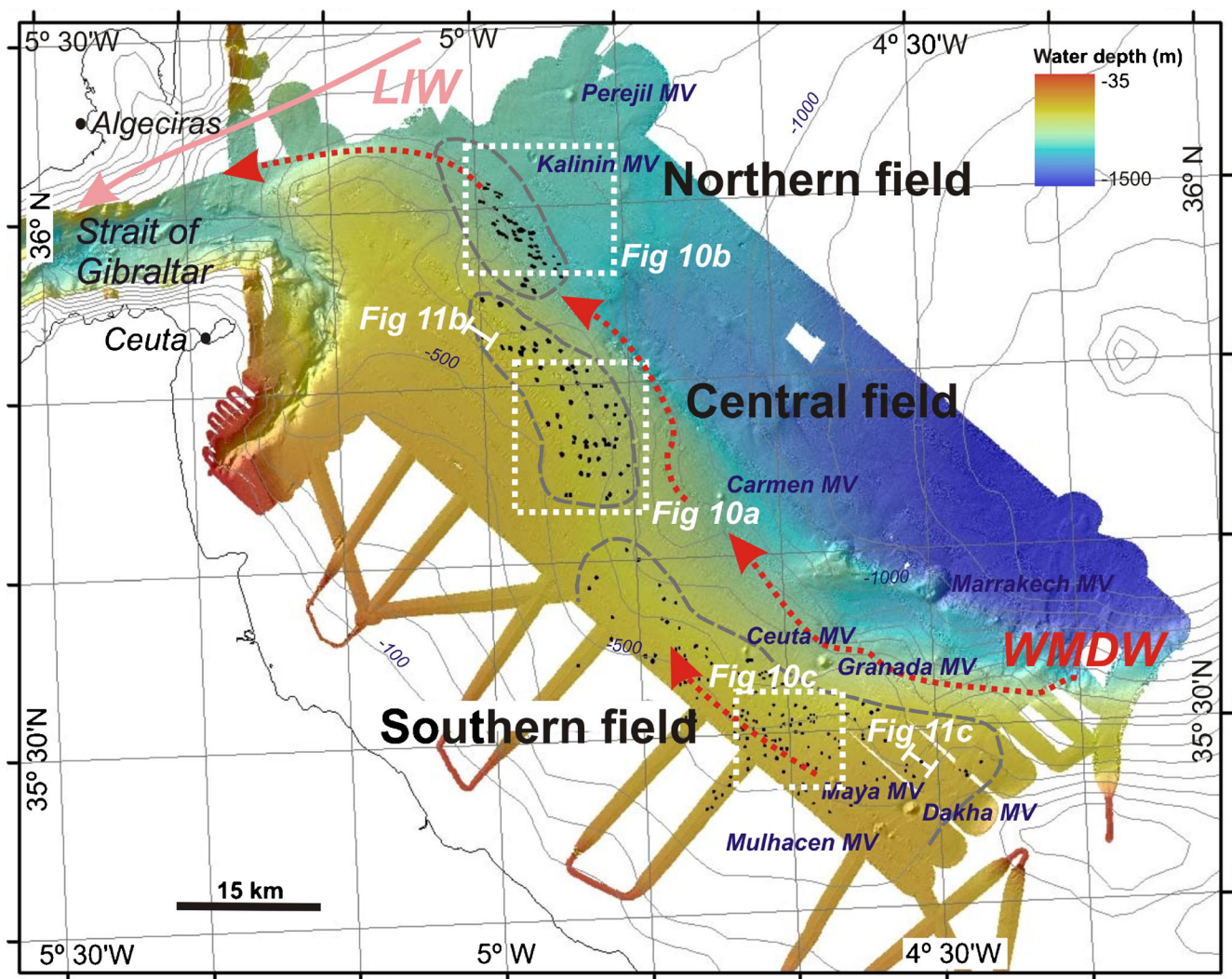


Fig. 8 Hillshade seafloor map generated from the 3D multibeam dataset acquired in the western Alborán Sea (Ceuta Drift): *black dots* pockmarks; *note grouping (grey dashed lines)* in the northern, central and southern fields. *MV* Mud volcanoes

Shallow subsurface contourite reservoirs

The formation of mud volcanoes as morphological expressions of hydrocarbon seeps in the WAB and the GoC has in the past been interpreted to be related to the upward migration of focused fluid flow from deep-seated reservoirs. In the GoC this was thought to be associated with thrust, extensional and strike-slip faults and diapirs (Pinheiro et al. 2003; Somoza et al. 2003; Medialdea et al. 2009), on the Ceuta Drift with shale diapirism (Pérez-Belzuz et al. 1997; Talukder et al. 2003; Blinova et al. 2011; Somoza et al. 2012). In the present study, by contrast, high-resolution seismic images have revealed that the pockmarks are not directly linked by feeder pipes to deep sources, but are instead connected to shallow subsurface reservoirs located within contourite deposits. In the Gulf of Cádiz and elsewhere, contourite drifts consist mainly of alternations of muddy–silty and sandy layers (high- and low-permeability sediments respectively) commonly (albeit

not always) reflecting fluctuating intensities of bottom currents (e.g. Faugères and Mulder 2011; Mulder et al. 2013). While the coarser-grained sediments can act as reservoirs for hydrocarbon-enriched fluids, overlying fine-grained sediments may act as effective seals (Viana 2008).

In the GoC, two of the pockmark fields, i.e. the main channel and TASYO fields, are clearly related to the MOW undercurrent. The main channel pockmarks are located above the sandy contourite terrace in the proximal sector of the GoC (Hernández-Molina et al. 2012). A dense field of HDAC chimneys and crusts was discovered and sampled during the TTR14 cruise along the border of the main channel (Blinova et al. 2006; Kozlova et al. 2006; Magalhães et al. 2012), related to hydrocarbon fluid venting in this area. Seismic images show a giant lenticular body interpreted as a palaeochannel (Fig. 6) formed in a period of intensified MOW undercurrent flow during the mid-Pleistocene revolution (Stow et al. 2011). Such palaeochannels are filled

Table 2 Main features and morphological parameters of the pockmark fields in the western Alborán area

Field	Western Alborán area			
		Northern	Central	Southern
Water depth (m)		714–880	466–597	379–587
Number		34	61	143
Area affected (km ²)		3	5.7	5
Density (m ² km ⁻²)		8,000–24,600	11,000–24,500	900–17,000
Shape		Elongated, lobate, merged	Isolated single, sub-circular, symmetrical, V-shaped	Isolated single, sub-circular, symmetrical, U-shaped
Depth (m)		3–15	15–30	0.5–1
Long axis (m)	Range	243–1,429	214–613	130–391
	Mode	500	400	235
Short axis (m)	Range	127–449	157–432	102–353
	Mode	280	290	187
Eccentricity (short axis/long axis)	Range	0.25–0.81	0.41–0.97	0.44–0.99
	Mode	0.4	0.8	0.9
Azimuth (°)	Range	82–143	0–180	0–180
	Mode	110	–	–
Slope (°)	Mean	1.5–4	6–15	1.2–1.8
	Max.	16	22	2.5
Seismics		Asymmetrical, eroded, underlain by transparent narrow funnel	Symmetrical, underlain by transparent narrow funnel	Symmetrical with thin pipe feeder covered by thin sediment layer
Statistical analyses				
Area range (km ²)		28–354	28–191	11–102
<i>A</i>		43	664	432
β exp-5		–1	–3	–6
Correlation coefficient		0.94	0.98	0.99

mainly by coarse-grained, high-porosity sands sealed by silty deposits and, hence, constitute excellent hydrocarbon reservoirs (Stow et al. 2011).

The pockmarks of the TASYO field, on the other hand, are located on a huge contourite levee generated by MOW overflow processes (Mulder et al. 2003). Fluid migration within these sandy contourite palaeo-levees is suggested as the main shallow subsurface fluid storage mechanism. In this case, pockmarks are intercalated between sand waves having exceptionally steep flanks (22–35°), suggesting that these may be freak sand waves sensu Judd and Hovland (2007), the oversteepening resulting from near-bottom flow modifications caused by active fluid seepage. The high slopes of the pockmarks are thus thought to be related to (1) removal of sediment by fluid flow, as proposed by Judd and Hovland (2007), and (2) high cohesion of the wall sediments due to cementation by HDACs, as observed at other sites of the TASYO field (e.g. Díaz-del-Río et al. 2003; Magalhães et al. 2012).

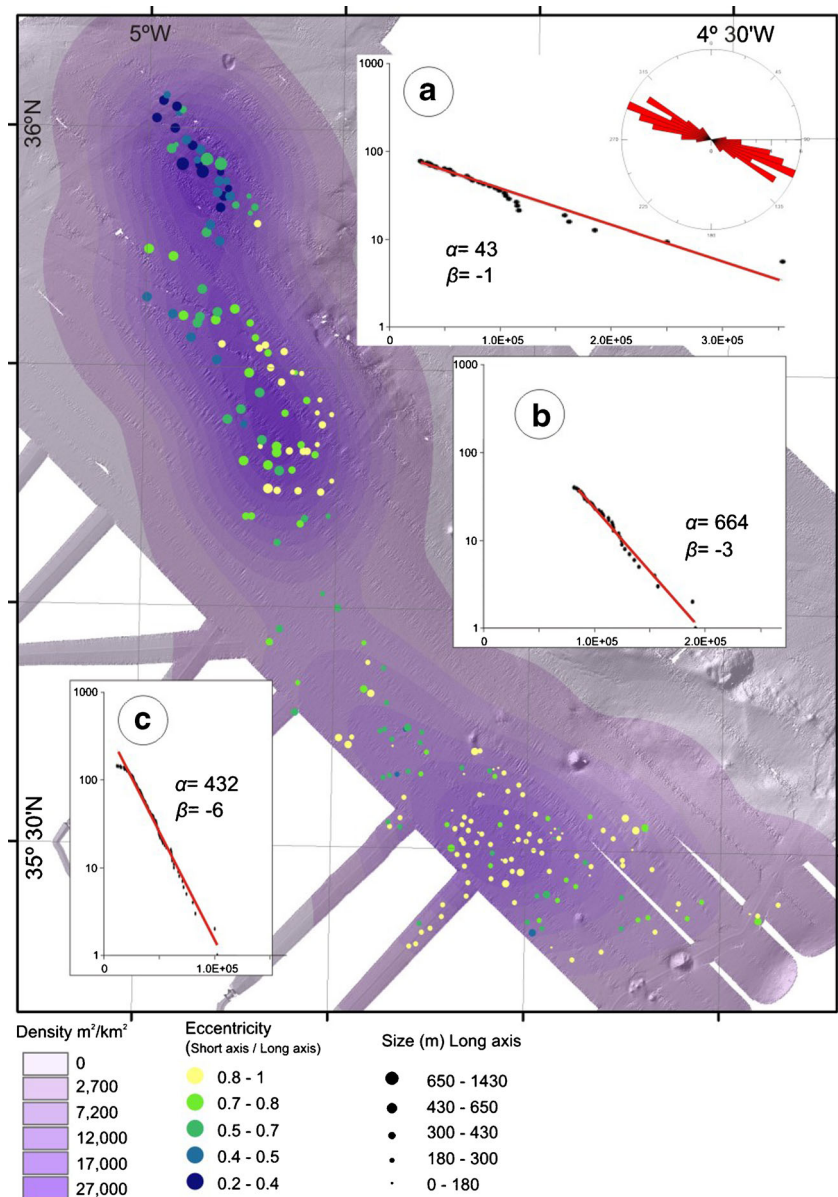
In the case of the upper slope field, the origin of subsurface reservoirs is not clear but could be related to alongslope migrating sand waves driven by NACW inflow through

the Strait of Gibraltar. The formation of gullies in this area points towards strong downslope currents which may have winnowed finer grain sizes, leaving behind coarser-grained deposits on the upper slope.

On the Mediterranean side of the strait, the Ceuta Drift pockmarks are interpreted to be related to shallow subsurface reservoirs controlled by grain-size variations (cf. Somoza et al. 2012). The sheet-like geometry of the plastered contourites dipping towards the basin facilitates upward migration of hydrocarbon-enriched fluids derived from the diapiric structures and mud volcano systems of the region, to generate shallow subsurface reservoirs within sandy lenses of the contourite deposits. Seepage from these reservoirs within the Ceuta Drift then generated fields of homogeneously distributed and similarly sized pockmarks.

Contrary to other types of fluid venting observed both in the GoC and the WAB, such as mud volcanoes or HDAC chimneys, the pockmarks identified in this study are not directly linked to deeper sources. Rather, they are sourced in shallow reservoirs formed as “second-generation” seeps derived from “primary” deep thermogenic gas-rich fluid

Fig. 9 Spatial distribution of pockmarks on the Ceuta Drift, western Alborán Basin, with cumulative size-frequency plots for the **a** northern, **b** central and **c** southern fields. For other information, see caption of Fig. 3. Note that a rose diagram showing the azimuths of the long axes was generated only for area **a** because eccentricity indices for the central and southern fields were close to 0.9



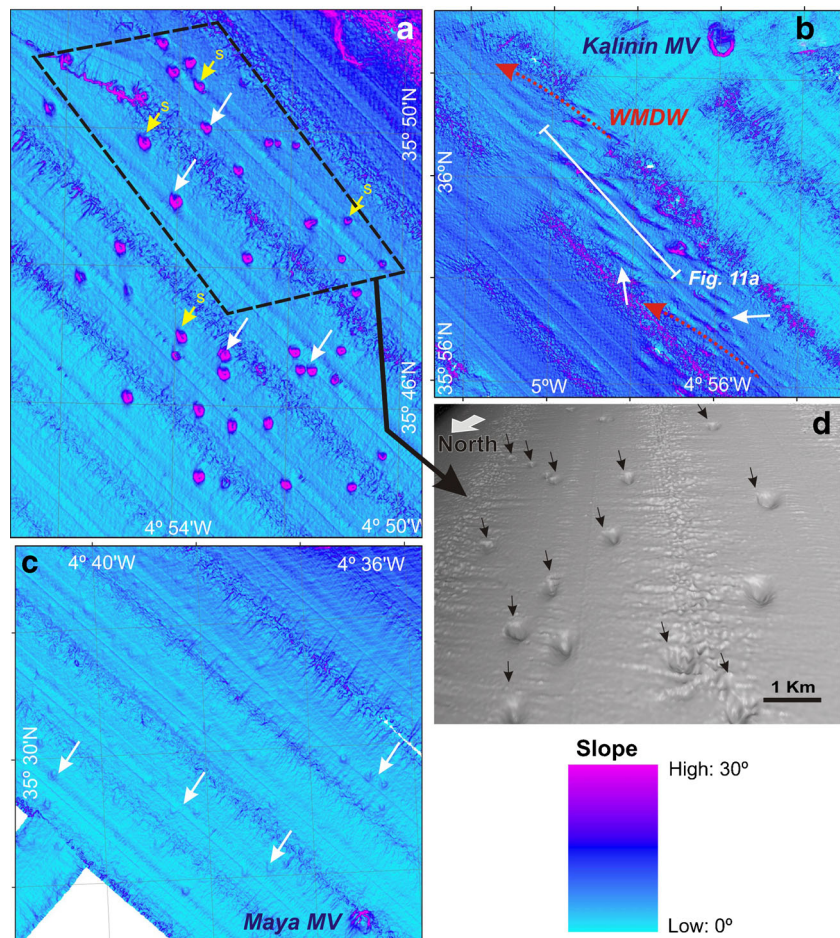
venting (Stadnitskaia et al. 2000, 2006) associated with marly diapirism of the Subbetic formations (Maldonado et al. 1999; Medialdea et al. 2004, 2009).

Trigger mechanisms

Gas hydrate dissociation has been proposed as the most probable mechanism for the formation of the pockmarks, collapse structures and blind valleys in the GoC at water depths greater than 800 m (León et al. 2010; León and Somoza 2011). However, at shallower depths in the Strait of Gibraltar, where the majority of pockmarks are located at water depths less than 550 m and hence exposed to the MOW undercurrent, hydrate dissociation is discarded as a viable trigger mechanism.

Instead, the mapping results and morphometric characterisation of the vast number of pockmarks on either side of the Strait of Gibraltar suggest a formation mechanism associated with the hydrodynamic regime in the strait. On this basis a hypothesis for the development of pockmarks on either side of the Strait of Gibraltar is proposed (Fig. 12), the main evidence being related to the fact that the pockmarks are associated with the first subsurface erosion surface which is overlain by a transparent layer representing the final transgressive Holocene deposit. The erosion surface below this transgressive deposit formed during the sea-level lowstand associated with the last glacial maximum (LGM; Figs. 5, 7, 11), when sea level on the continental shelf of the GoC is estimated to have stood 120 m below the present-day level (Somoza et al. 1997). This dramatic sea-level lowering affected the stability of the

Fig. 10 Seabed dip map showing the distribution and morphology of pockmarks (*arrows*) in the central, northern and southern fields. **a** Central field: *s* locally smooth profiles. **b** Northern field, and the location of the chirp profile reported in Fig. 11a. **c** Southern field. **d** Hillshade map of the central field (Ceuta Drift) imaging the random distribution and morphology of sub-circular and elongated pockmarks



shallow hydrocarbon reservoirs in two ways: (1) by reducing the effective hydrostatic pressure above the overpressured pore water in the sediment, upward migration of gas-charged fluids to the seafloor was promoted, and (2) an increase in the MOW volume and velocity (Hernández-Molina et al. 2006), caused by a lowering of the Atlantic sea level relative to that of the Mediterranean, favoured the formation of large internal waves which were, in addition, amplified by the emergent topography in the Strait of Gibraltar (Gasser et al. 2011; Fig. 12a). Likewise, the distribution of pockmarks on the Ceuta Drift, although random, also appears to be related to the shape of modern internal waves deflected at the entry to the Mediterranean Sea (Figs. 1, 12). This suggests a potential influence of this hydrodynamic process on their formation.

The decrease in hydrostatic pressure during the sea-level lowstand resulted in the expansion of sediment-trapped bubbles within the shallow subsurface reservoirs. At the same time, rhythmic tidal water level changes and large internal waves acted as “hydraulic pumps” of the shallow subsurface free gas accumulations, causing small amounts of sediment pore water to be periodically pumped out of the seafloor, the venting process resulting in the formation of pockmarks. The proposed mechanism is very similar to the tidal pumping

regime described by Hovland et al. (1999) from the Norwegian continental margin. Furthermore, the increase in intensity of the undercurrent above the pockmarks would have produced a positive vertical current component (Hammer et al. 2009; Pau et al. 2014, and references therein) which may have reinforced the pumping effect of the internal waves.

According to the above hypothesis, the formation of pockmarks on either side of the Strait of Gibraltar thus took place during various phases of late Pleistocene sea-level fluctuations in relation to the exchange of water masses between the Atlantic and the Mediterranean. Thus, on the Atlantic side of the strait, the periods of maximum hydraulic activity were associated with a number of regressive phases. Together with decreases in hydrostatic pressure, the generation of large turbulent eddies (Fig. 12a) caused by the increasing intensity of the high-density MOW undercurrent resulted in the formation of pockmarks. This interpretation is supported by ultrahigh-resolution seismic profiles which revealed the occurrence of several stacked erosional discontinuities on the slope of the GoC (Fig. 5). These erosion surfaces were probably caused by four punctuated forced regressive episodes affecting the shelf and slope of the Gulf of Cádiz following the sea-level highstands dated at 140–120, 105–100 and 70–

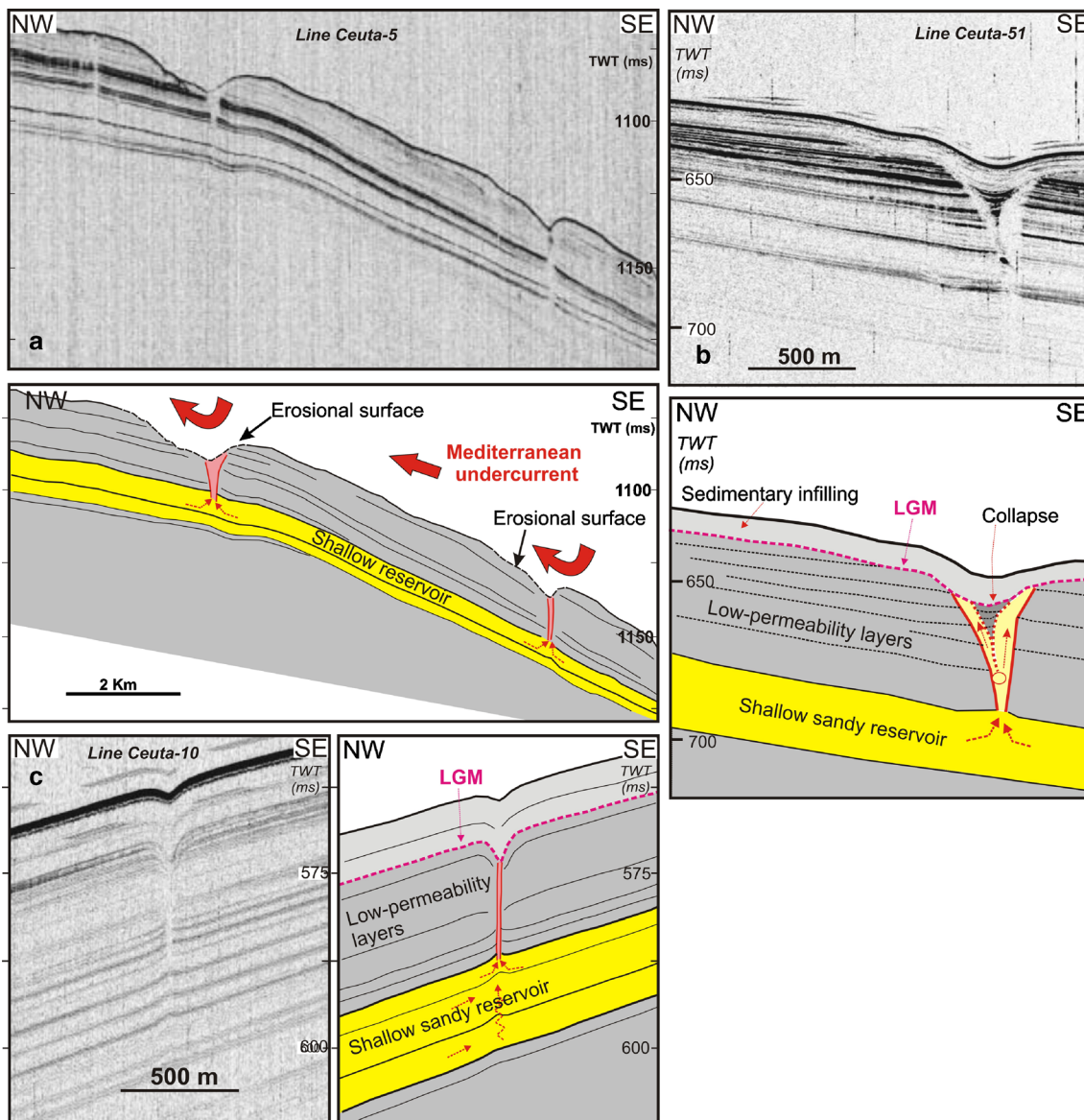


Fig. 11 Chirp profiles showing cross sections of the Ceuta Drift. **a** Northern field, TOPAS seismic line Ceuta-5: pockmarks with an asymmetrical V-shaped erosional depression underlain by an acoustically transparent, narrow funnel rooted in a shallow reservoir. See Fig. 10b for location. **b** Central field, TOPAS seismic line Ceuta-51: acoustically

transparent, narrow funnel-rooted pockmark with symmetrical V-shaped depression. **c** Southern field, TOPAS seismic line Ceuta-10: symmetrical V-shaped pockmark over a narrow pipe-shaped feeder covered by a thin sediment layer. **b** and **c** See Fig. 8 for location

80 ka BP, as well as during marine isotope stage 3 (Somoza et al. 1997).

On the Mediterranean side of the strait, by contrast, the maximum hydraulic activity is related to the onset of the transgression after the last sea-level lowstand when the abrupt sea-level rise generated rapid inflow of Atlantic mass waters into the Mediterranean Sea (Fig. 12b). The pumping effect caused by the amplification of internal waves formed at the interface between the water masses can explain the formation of the pockmarks on the Ceuta Drift immediately after the last sea-level lowstand. Thus,

the pockmarks in the WAB would have formed after the LGM due to the increase of Atlantic water inflow into the Mediterranean. Evidence for this is again provided by ultrahigh-resolution seismic profiles which show that the pockmarks in this region are related to a single erosional discontinuity interpreted to represent the LGM (Figs. 5, 10, 11). Whereas the pockmarks of the southern field are almost entirely draped by transgressive contourite sediments, those of the northern field are at present affected by erosion processes (Fig. 11a), which resulted in their high degree of elongation (Table 2) and asymmetry

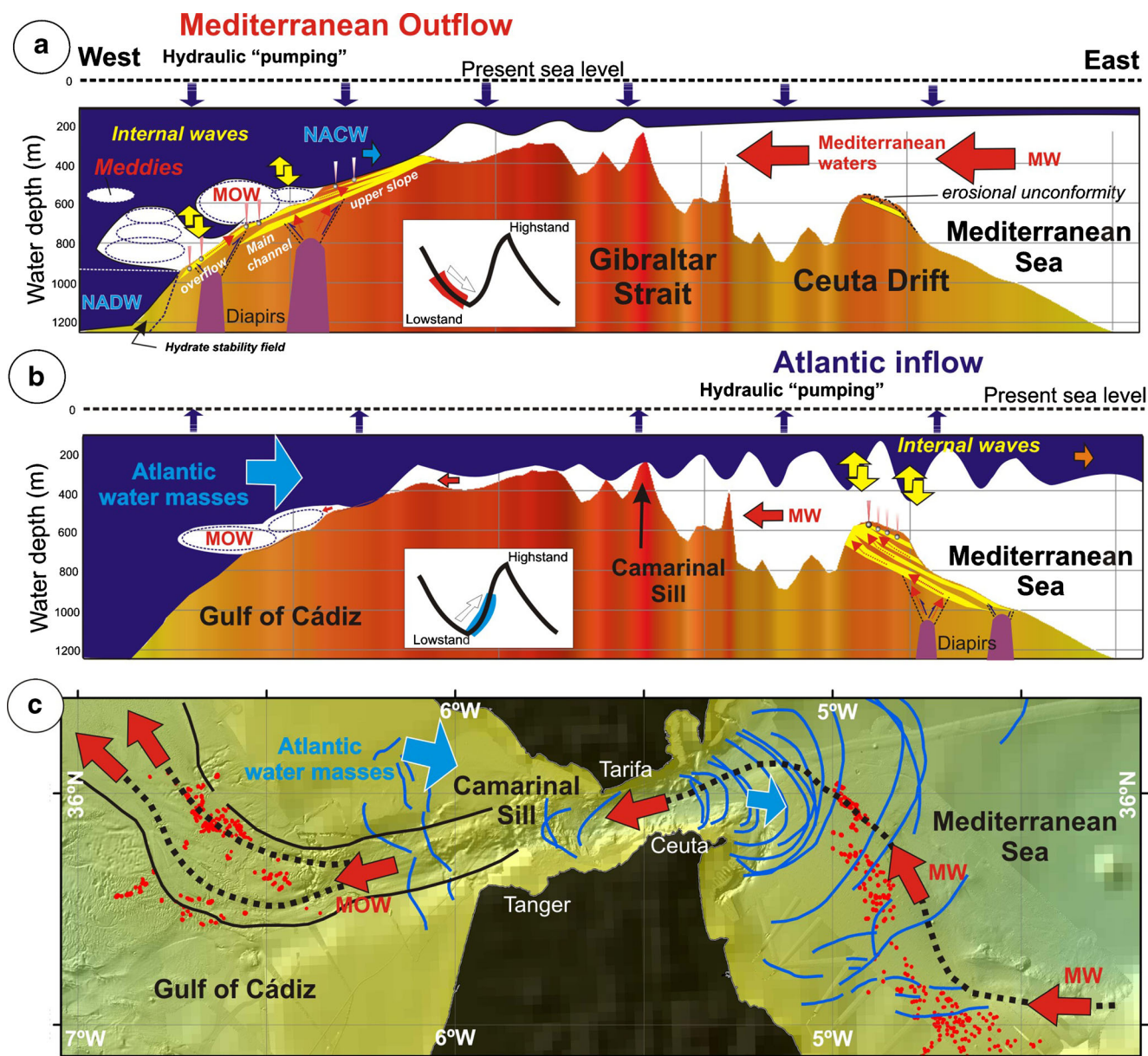


Fig. 12 Model proposed for pockmark development on either side of the Strait of Gibraltar in relation to the formation of large-amplitude internal waves generated along the interface between Mediterranean and Atlantic waters. **a** Formation of pockmarks in the Gulf of Cádiz during maximum outflows of Mediterranean water masses. During the subsequent sea-level fall prior to the lowstand, the increase in the volume and the higher velocity of the Mediterranean outflow may have resulted in the overflow of the main contourite channel in the Gulf of Cádiz. **b** Formation of

pockmarks in the western Alborán Basin during maximum inflows of Atlantic water in relation to periods of rapid sea-level rise after the lowstand. **c** Mapping of pockmarks (red dots) and circulation pattern of Mediterranean and Atlantic water masses (red and blue arrows respectively). Superimposed (arcuate blue lines) are examples of modern internal waves generated along the interface between Atlantic and Mediterranean water masses (modified from Jackson 2004)

reflecting the direction of bottom-current flow across the Ceuta Drift (Figs. 9a and 10b).

Morphology vs. fluid flow and oceanography

Studies of volcanic cinder edifices have shown that monogenic morphologies follow a single logarithmic trend reflected by similar β values (Pérez-López et al.

2011). In this sense, a population of pockmarks with different β values would be related to different genetic processes. In this paper, the morphological analyses of pockmarks show different shapes, typologies, density, and distribution patterns in the study areas. These differences are interpreted to reflect different geological and/or oceanographic processes in their generation. The pockmarks have accordingly been grouped into a

number of fields having different morpho-structural characteristics and logarithmic trends.

In the GoC, pockmarks are scarce and restricted to three well localized and separated high-density fields (Fig. 3). The upper slope field has two different logarithmic trends (Table 1). Small pockmarks (β of -2) are directly related to gas venting processes, whereas the larger ones (β of -1), which have the same alignment as the gullies (45°N), show an overprint of at least two processes, namely fluid flow and gully erosion.

In the main channel field, the pockmarks are concentrated in the western sector of the field on top of contourite deposits, but are absent where rocks of the Flysh Complex crop out. They are NW–SE aligned, matching the direction of buried channels within which shallow hydrocarbon reservoirs are located. Two populations can be geographically separated in this field: a northern (with the majority of pockmarks) and a southern branch (Fig. 3), each one probably indicative of a buried channel beneath. On account of the larger number of pockmarks, the northern branch may be associated with a better developed reservoir containing more gas. In analogy to the upper slope field, the statistical morphological analysis shows two different logarithmic trends (Fig. 3): one for the small sizes (β of -3) and another for the large ones (β of -1). The small sub-circular features are thought to be related to gas-rich fluid venting, whereas the bi-modally distributed (azimuths of 56°N and 135°N) elongated larger ones reflect a combination of tectonic (trending 56°N) and MOW erosion (135°N) processes.

In the WAB, the pockmark density map shows a single large cluster composed of three interconnected core regions corresponding to the three described fields. The statistical morphological analysis reveals a different logarithmic trend in each case, i.e. β of -1 , -3 and -6 for the northern, central and southern field respectively. The elongated morphologies of the northern field seem to be related to the interaction between the flow of the WMDW and the surface of the Ceuta Drift. The observed merging of pockmarks was probably caused by erosion to form lobate and elongated pockmarks or furrows (Fig. 10b). The morphologies produced by undercurrent activity (northern field in WAB and US 2, Table 2; MC 2 in GoC, Table 1) thus show large elongated sizes and a characteristic high β value of -1 .

With respect to the distinct β values of the central and southern fields, the trends in size and eccentricity may point to other pockmark formation processes. Seismic profiles show different features in the individual fields, sedimentary infillings being related to the oceanographic regime, feeder channels to fluid flow mechanisms. These may have resulted from variations in sediment composition or from different effective hydrostatic pressures at the seafloor (related to internal waves) in relation to their respective distance from the Strait of Gibraltar.

Conclusions

- In all, 436 pockmarks have for the first time been mapped in detail in two areas on either side of the Strait of Gibraltar by means of multibeam bathymetry and high-resolution seismics. Of these, 198 pockmarks have been newly identified in the Gulf of Cádiz (Atlantic side) and 238 in the western Alborán Basin (Mediterranean side).
- In the Gulf of Cádiz, pockmarks occur in three well localized and separated fields related to Mediterranean water outflow, i.e. the upper slope, main channel and TASYO fields. The pockmarks are at 450–1,020 m water depths and have sub-circular to irregular elongated shapes. The majority (160) are elongated, being located along the main channel of the Mediterranean outflow undercurrent.
- In the western Alborán Basin, pockmarks are distributed across three interconnected fields, i.e. a northern, a central and a southern field. A total of 238 randomly distributed pockmarks (130–1,430 m in diameter) occur at water depths of 370–880 m, most being sub-circular with an average diameter of 400 m. The pockmarks of the northern field, located close to the entrance to the Strait of Gibraltar, are the largest and have elongated shapes. On seismic profiles, the pockmarks appear as vertical funnels and columnar disturbances overlain by thin packages of parallel reflectors concordant with the seabed.
- The pockmarks are related to the venting of overpressured gas-rich fluid entrapped in shallow subsurface reservoirs consisting of coarse-grained contourites deposited in mid-Pleistocene palaeochannels and levees charged by deep-seated fluids migrating upwards along diapir-related faults.
- Based on their seismo-stratigraphic position associated with the last erosional discontinuity below Holocene transgressive deposits, it is inferred that the pockmarks must have formed during the last glacial sea-level lowstand (late Pleistocene).
- It is proposed that release of gas from subsurface reservoirs occurred during the last sea-level lowstand, characterised by strong water exchanges between the Mediterranean and the Atlantic. A strong drop in sea level would have reduced the effective hydrostatic pressure, resulting in overpressured sediment pore water and thereby favouring an upward migration of gas-rich fluids. This would have been further promoted by the formation of large internal waves amplified by the emergent topography in the Strait of Gibraltar during the last sea-level lowstand, which would act as “hydraulic pumps” for the shallow subsurface free gas accumulations.
- Release of gas-rich fluid from shallow reservoirs worldwide may thus have been increased during sea-level

lowstands due to effects of both strong deepwater undercurrents and internal waves. The mechanism proposed here for the formation of hydraulic pockmarks on either side of the Strait of Gibraltar is similar to the tidal pumping suggested for other oceanographic settings.

Acknowledgements This work has been supported by the Spanish projects CONTOURIBER (CTM 2008-06399-C04/MAR) and SUBVENT (CGL2012-39524-C02). We thank two anonymous reviewers for thorough assessments which helped improve the article.

References

- Ambar I, Howe MR (1979) Observations of the Mediterranean outflow—II. The deep circulation in the vicinity of the Gulf of Cadiz. *Deep-Sea Res I* 26:555–568
- Ambar I, Serra N, Brogueira MJ, Cabeçadas G, Abrantes F, Freitas P, Gonçalves C, Gonzalez N (2002) Physical, chemical and sedimentological aspects of the Mediterranean outflow off Iberia. *Deep-Sea Res I* 49:4163–4177
- Baraza J, Ercilla G (1996) Gas-charged sediments and large pockmark like features on the Gulf of Cadiz slope (SW Spain). *Mar Petrol Geol* 13(2):253–261
- Blinova VN, Ivanov MK, Pinheiro LM (2006) Underwater video observations. In: Kenyon NH, Ivanov MK, Akhmetzhanov AM, Kozlova EV (eds) *Interdisciplinary geoscience studies of the Gulf of Cadiz and Western Mediterranean Basins*. Preliminary results of investigations during the TTR-14 cruise of RV Professor Logachev, July–September, 2004. IOC Tech Series 70:24–30
- Blinova VN, Comas MC, Ivanov MK, Poludetkina EN, Matveeva TV (2011) Active mud volcanism in the West Alborán Basin: geochemical evidence of hydrocarbon seepage. *Mar Petrol Geol* 28:1483–1504
- Bøe R, Rise L, Ottesen D (1998) Elongate depressions on the southern slope of the Norwegian trench (Skagerrak): morphology and evolution. *Mar Geol* 146:191–203
- Brackenridge R, Stow DAV, Hernández-Molina FJ (2011) Contourites within a deep-water sequence stratigraphic framework. *Geo-Mar Lett* 31(5/6):343–360. doi:10.1007/s00367-011-0256-9
- Brothers LL, Kelley JT, Belknap DF, Barnhardt WA, Andrews BD, Maynard ML (2011) More than a century of bathymetric observations and present-day shallow sediment characterization in Belfast Bay, Maine, USA: implications for pockmark field longevity. *Geo-Mar Lett* 31(4):237–248. doi:10.1007/s00367-011-0228-0
- Bruno M, Alonso JJ, Cózar A, Vidal J, Echevarría F, Ruiz J, Ruiz-Cañavate (2002) The boiling water phenomena at Camarinal sill, the Strait of Gibraltar. *Deep-Sea Res II* 49:4097–4113
- Buitrago J, García C, Cajebread-Brow J, Jiménez A, Martínez del Olmo W (2001) Contourites: un excelente almacén casi desconocido (Golfo de Cádiz, SO de España). In: *Ext Abstr Vol Congr Técnico Exploración y Producción REPSOL-YPF*, 24–27 September 2001, Madrid
- Cathles LM, Su Z, Chen D (2010) The physics of gas chimney and pockmark formation, with implications for assessment of seafloor hazards and gas sequestration. *Mar Petrol Geol* 27:82–91
- Çifçi G, Dondurur D, Ergün M (2003) Deep and shallow structures of large pockmarks in the Turkish shelf, Eastern Black Sea. *Geo-Mar Lett* 23(3/4):311–322. doi:10.1007/s00367-003-0138-x
- Comas MC, García-Dueñas V, Jurado MJ (1992) Neogene tectonic evolution of the Alboran Sea from MCS data. *Geo-Mar Lett* 12:157–164. doi:10.1007/BF02084927
- Comas MC, Soto JI, Talukder AR, TTR-12 Leg 3 (Marsibal-1) Scientific Party (2003) Discovering active mud volcanoes in the Alboran Sea (Western Mediterranean). In: Marani M, Akhmanov G, Suzumov A (eds) *Geological and biological processes at deep-sea European margins and oceanic basins*. Int Conf and 11th Post-Cruise Meet TTR Programme, 2–6 February 2003, Bologna. IOC Worksh Rep 220:14–16
- Dando PR, Hovland M (1992) Environmental effects of submarine seeping natural gas. *Cont Shelf Res* 12:1197–1207
- Díaz-del-Río V, Somoza L, Matínez-Frías J, Mata MP, Delgado A, Hernández Molina FJ, Lunar R, Martín Rubí JA, Maestro A, Fernández Puga MC, León R, Llave E, Medialdea T, Vázquez JT (2003) Vast field of hydrocarbon-derived carbonate chimneys related to the accretionary wedge/olistostrome of the Gulf of Cadiz. *Mar Geol* 195:177–200
- Eichhubl P, Greene HG, Naehr T, Maher N (2000) Structural control of fluid flow: offshore seepage in the Santa Barbara Basin, California. *J Geochem Explor* 69(70):545–549
- Ercilla G, Baraza J, Alonso B, Estrada F, Casas D, Farrán M (2002) The Ceuta Drift, Alboran Sea, southwestern Mediterranean. In: Stow DAV, Pudsey CJ, Howe JA, Faugères JC, Viana AR (eds) *Deep water contourites systems: Modern drifts and ancient series, seismic and sedimentary characteristics*. *Geol Soc Lond Mem* 22:155–170
- Esteras M, Izquierdo J, Sandoval NG, Bahmad A (2000) Evolución morfológica y estratigráfica pliocuaternaria del Umbral de Camarinal (Estrecho de Gibraltar) basada en sondeos marinos. *Rev Soc Geol España* 13:539–550
- Faugères J-C, Mulder T (2011) Contour currents and contourite drifts. In: Hüneke H, Mulder T (eds) *Deep-sea sediments, Developments in Sedimentology*, vol. 63. Elsevier, Amsterdam, pp 149–214
- Faugères JC, Gonthier E, Stow DAV (1984) Contourite drift molded by deep Mediterranean outflow. *Geology* 12:296–300
- Fernández-Puga MC, Vázquez JT, Somoza L, Díaz del Río V, Medialdea T, Mata MP, León R (2007) Gas-related morphologies and diapirism in the Gulf of Cádiz. *Geo-Mar Lett* 27(2/4):213–221. doi:10.1007/s00367-007-0076-0
- Foucher J-P, Westbrook GK, Boetius A, Ceramicola S, Dupré S, Mascle J, Mienert J, Pfannkuche O, Pierre C, Praeg D (2009) Structure and drivers of cold seep ecosystems. *Oceanography* 22:92–109
- Gardner JM (2001) Mud volcanoes revealed and sampled on the Western Moroccan continental margin. *Geophys Res Lett* 28(2):339–342
- Gasser M, Pelegrí JL, Nash JD, Peters H, García-Lafuente J (2011) Topographic control on the nascent Mediterranean outflow. *Geo-Mar Lett* 31(5/6):301–314. doi:10.1007/s00367-011-0255-x
- Gay A, Lopez M, Cochonat P, Sermondadaz G (2004) Polygonal faults-furrows system related to early stages of compaction—Upper Miocene to present sediments of the Lower Congo Basin. *Basin Res* 16:101–116
- González FJ, Somoza L, León R, Medialdea T, Torres T, Ortiz JE, Lunar R, Martínez-Frías J, Merinero R (2012) Ferromanganese nodules and micro-hardgrounds associated with the Cadiz Contourite Channel (NE Atlantic): palaeoenvironmental records of fluid venting and bottom currents. *Chem Geol* 310(311):56–78
- Habgood EL, Kenyon NH, Masson DG, Akhmetzhanov A, Weaver PPE, Gardner J, Mulder T (2003) Deep-water sediment wave fields, bottom current sand channels and gravity flow channel lobe system: Gulf of Cadiz, NE Atlantic. *Sedimentology* 50:483–510
- Hammer Ø, Webb KE, Depreiter D (2009) Numerical simulation of upwelling currents in pockmarks, and data from the Inner Oslofjord, Norway. *Geo-Mar Lett* 29(4):269–275. doi:10.1007/s00367-009-0140-z
- Hanquiez V, Mulder T, Lecroart P, Gonthier E, Marchès E, Voisset M (2007) High resolution seafloor images in the Gulf of Cádiz, Iberian margin. *Mar Geol* 246:42–59

- Hernández-Molina FJ, Llave E, Somoza L, Fernández-Puga MC, Maestro A, León R, Medialdea T, Barnolas A, García M, Díaz-del-Río V, Fernández-Salas LM, Vázquez JT, Lobo FJ, Alveirinho-Dias JA, Rodero J, Gardner J (2003) Looking for clues to paleoceanographic imprints: a diagnosis of the Gulf of Cadiz contourite depositional systems. *Geology* 31:19–22
- Hernández-Molina FJ, Llave E, Stow DAV, García M, Somoza L, Vázquez JT, Lobo FJ, Maestro A, Díaz-del-Río V, León R, Medialdea T, Gardner J (2006) The contourite depositional system of the Gulf of Cadiz: a sedimentary model related to the bottom current activity of the Mediterranean outflow water and its interaction with the continental margin. *Deep-Sea Res II* 53:1420–1463
- Hernández-Molina FJ, Llave E, Stow DAV (2008) Continental slope contourites. In: Rebesco M, Camerlenghi A (eds) *Contourites, Developments in Sedimentology*, vol. 60. Elsevier, Amsterdam, pp 379–407
- Hernández-Molina FJ, Serra N, Stow DAV, Llave E, Ercilla G, Van Rooij D (2011) Along-slope oceanographic processes and sedimentary products around the Iberian margin. *Geo-Mar Lett* 31(5/6):315–341. doi:10.1007/s00367-011-0242-2
- Hernández-Molina FJ, Llave E, Fontan A, Brackenridge RE, Stow DAV, Ercilla G, Medialdea T, García M, Sandoval N, Preu B, Arlucea MP, Nombela MA, Alejo I, Francés G, Mena A, Casas D, Somoza L, León R, Vázquez JT, Juan C, Van Rooij D, Matias H, Bruno M, Serra N, Team CONTOURIBER (2012) First evidence of a main channel generated by the Mediterranean Outflow Water after its exit from the Gibraltar Strait. *Geo-Temas* 13:1813–1816
- Hovland M, Judd A (1988) Seabed pockmarks and seepages. Impact on geology, biology and the marine environment. Graham and Trotman, London
- Hovland M, Løseth H, Bjørkum PA, Wensaas L, Arntsen B (1999) Seismic detection of shallow high pore pressure zones. *Offshore*, Dec., pp 94–96
- Hovland M, Svensen H, Forsberg CF, Johansen H, Fichler C, Fosså JH, Jonsson R, Rueslåtten H (2005) Complex pockmarks with carbonate-ridges off mid-Norway: products of sediment degassing. *Mar Geol* 218:191–206
- Hovland M, Heggland R, De Vries MH, Tjelta TI (2010) Unit-pockmarks and their potential significance for predicting fluid flow. *Mar Petrol Geol* 27:1190–1199
- Hovland M, Jensen S, Indreiten T (2012a) Unit pockmarks associated with *Lophelia* coral reefs off mid-Norway: more evidence of ‘fertilizing’ bottom currents. *Geo-Mar Lett* 32(5/6):545–554. doi:10.1007/s00367-012-0284-0
- Hovland M, Jensen S, Fichler C (2012b) Methane and minor oil macroseep systems—their complexity and environmental significance. *Mar Geol* 332(334):163–173
- Ivanov MK, Kenyon N, Nielsen T, Wheeler A, Monteiro H, Gardner J, Comas M, Akhmanov A, Akhmetzhanov G (2000) Goals and principal results of the TTR-9 cruise. *IOC/UNESCO Worksh Rep* 168:3–4
- Ivanov M, Pinheiro LM, Stadnitskaia A, Blinova V (2001) Hydrocarbon seeps on the deep Portuguese margin. In: *Abstr Vol European Union of Geosciences Meeting, EUG XI*, 8–12 April 2001, Strasbourg, p 105
- Ivanov MK, Kenyon NH, Laberg JS, Blinova VN (2010) Cold seeps, coral mounds and deep-water depositional systems of the Alborán Sea, Gulf of Cadiz and Norwegian Continental Margin. Preliminary results of investigations during the TTR-17 cruise of RV Professor Logachev, June–July, 2008. *IOC Tech Series* 94
- Jackson CR (2004) The Strait of Gibraltar. In: *An atlas of internal solitary-like waves and their properties*. Global Ocean Associates. Office of Naval Research (Code 322PO), pp 179–198
- Judd A, Hovland M (2007) *Seabed fluid flow: the impact on geology, biology and the marine environment*. Cambridge University Press, Cambridge
- Kelley JT, Dickson SM, Belknap DF, Barnhardt WA, Henderson M (1994) Giant sea-bed pockmarks: evidence for gas escape from Belfast Bay. *Mar Geol* 22(1):59–62
- Kenyon NH, Ivanov MK, Akhmetzhanov AM, Akhmanov GG (2000) Multidisciplinary study of geological processes on the North East Atlantic and Western Mediterranean Margins. Preliminary results of geological and geophysical investigations during the TTR-9 cruise of R/V Professor Logachev, June–July, 1999. *IOC Tech Series* 56. UNESCO, Paris
- Kenyon NH, Ivanov MK, Akhmetzhanov AM, Akhmanov GG (2003) Interdisciplinary geoscience research on the North East Atlantic Margin Mediterranean Sea and Mid-Atlantic Ridge during the TTR-12 cruise of RV Professor Logachev, June–August 2001. *IOC Tech Series* 67. UNESCO, Paris
- Kenyon NH, Ivanov MK, Akhmetzhanov AM, Kozlova EV (2006) Interdisciplinary geoscience studies of the Gulf of Cadiz and Western Mediterranean Basins. Preliminary results of investigations during the TTR-14 cruise of RV Professor Logachev, July–September, 2004. *IOC Tech Series* 70
- Kozlova E, Sarantsev E, Bileva E, Blinova V, Korost D, Ovsyannikov V, Logvina E, Shuvalov A et al. (2006) Bottom sampling results. In: Kenyon NH, Ivanov MK, Akhmetzhanov AM, Kozlova EV (eds) *Interdisciplinary geoscience studies of the Gulf of Cadiz and Western Mediterranean Basins. Preliminary results of investigations during the TTR-14 cruise of RV Professor Logachev, July–September, 2004*. *IOC Tech Series* 70:31–37
- León R, Somoza L (2011) GIS-based mapping for marine geohazards in seabed fluid leakage areas (Gulf of Cadiz, Spain). *Mar Geophys Res* 32:207–223
- León R, Somoza L, Medialdea T, Maestro A, Díaz-del-Río V, Fernández-Puga MC (2006) Classification of sea-floor features associated with methane seeps along the Gulf of Cádiz continental margin. *Deep-Sea Res II* 53:1464–1481
- León R, Somoza L, Medialdea T, Hernández-Molina FJ, Vázquez JT, Díaz-del-Río V, González FJ (2010) Pockmarks, collapses and blind valleys in the Gulf of Cádiz. *Geo-Mar Lett* 30(3/4):231–247. doi:10.1007/s00367-009-0169-z
- León R, Somoza L, Medialdea T, Vázquez JT, González FJ, López-González N, Casas D, Mata MP, Fernández-Puga MC, Giménez-Moreno CJ, Díaz-del-Río V (2012) New discoveries of mud volcanoes on the Moroccan Atlantic continental margin (Gulf of Cádiz): morpho-structural characterization. *Geo-Mar Lett* 32(5/6):473–488. doi:10.1007/s00367-012-0275-1
- Magalhães VH, Pinheiro LM, Ivanov MK, Kozlova E, Blinova V, Kolganova J, Vasconcelos C, McKenzie JA, Bernasconi SM, Kopf A, Díaz-del-Río V, González FJ, Somoza L (2012) Formation processes of methane-derived authigenic carbonates from the Gulf of Cadiz. *Sediment Geol* 243(244):155–168
- Maldonado A, Somoza L, Pallares L (1999) The Betic orogen and the Iberian-African boundary in the Gulf of Cadiz: geological evolution (central North Atlantic). *Mar Geol* 155:9–43
- Medialdea T, Vegas R, Somoza L, Vázquez JT, Maldonado A, Díaz-del-Río V, Maestro A, Córdoba D, Fernández-Puga MC (2004) Structure and evolution of the “Olistostrome” complex of the Gibraltar Arc in the Gulf of Cádiz (eastern Central Atlantic): evidence from two long seismic cross sections. *Mar Geol* 209:173–198
- Medialdea T, Somoza L, Pinheiro LM, Fernández-Puga MC, Vázquez JT, León R, Ivanov MK, Magalhães V, Díaz-del-Río V, Vegas R (2009) Tectonics and mud volcano development in the Gulf of Cádiz. *Mar Geol* 261:48–63
- Millot C (1999) Circulation in the Western Mediterranean Sea. *J Mar Syst* 20(1/4):423–442
- Mulder T, Voisset M, Lecroart P, Le Drezen E, Gonther E, Hanquiez V, Faugères J-C, Habgood E, Hernandez-Molina FJ, Estrada F, Llave-Barranco E, Poirier D, Gorini C, Fuchey Y, Voelker A, Freitas P,

- Lobo Sanchez F, Fernandez LM, Kenyon NH, Morel J (2003) The Gulf of Cadiz: an unstable giant contouritic levee. *Geo-Mar Lett* 23: 7–18. doi:10.1007/s00367-003-0119-0
- Mulder T, Hassan R, Ducassou E, Zaragosi S, Gonthier E, Hanquiez V, Marchès E, Toucanne S (2013) Contourites in the Gulf of Cadiz: a cautionary note on potentially ambiguous indicators of bottom current velocity. *Geo-Mar Lett* 33(5):357–367. doi:10.1007/s00367-013-0332-4
- Nakamura T, Awaji T (2001) A growth mechanism for topographic internal waves generated by an oscillatory flow. *J Phys Oceanogr* 31:2511–2524
- Ondréas H, Olu K, Fouquet Y, Charlou JL, Gay A, Dennielou B, Donval JP, Fifis A, Nadalig T, Cochonat P, Cauquil E, Bourillet JF, Le Moigne M, Sibuet M (2005) ROV study of a giant pockmark on the Gabon continental margin. *Geo-Mar Lett* 25(5):281–292. doi:10.1007/s00367-005-0213-6
- Pau M, Gisler G, Hammer Ø (2014) Experimental investigation of the hydrodynamics in pockmarks using particle tracking velocimetry. *Geo-Mar Lett* 34(1):11–19. doi:10.1007/s00367-013-0348-9
- Paull C, Dillon WP (2001) Natural gas hydrates: occurrence, distribution and detection. *Geophys Monogr Ser* 124
- Pérez-Belzuz F, Alonso B, Ercilla G (1997) History of mud diapirism and trigger mechanisms in the Western Alborán Sea. *Tectonophysics* 282:399–422
- Pérez-López R, Legrand D, Garduño-Monroy VH, Rodríguez-Pascua MA, Giner-Robles JL (2011) Scaling laws of the size-distribution of monogenetic volcanoes within the Michoacán-Guanajuato Volcanic Field (Mexico). *J Volcanol Geotherm Res* 201:65–72
- Pinheiro LM, Ivanov MK, Sautkin A, Akhmanov G, Magalhães VH, Volkonskaya A, Monteiro JH, Somoza L, Gardner J, Hamouni N, Cunha MR (2003) Mud volcanism in the Gulf of Cadiz: results from the TTR-10 cruise. *Mar Geol* 195:131–151
- Poludetskina E, Kozlova E (2003) Geochemical characteristics of hydrocarbon gases and organic matter from mud volcanic deposits of the Alboran Sea. In: Marani M, Akhmanov G, Suzyumov A (eds) Geological and biological processes at deep-sea European margins and oceanic basins. *Int Conf and 11th Post-Cruise Meeting TTR Programme*, 2–6 February 2003, Bologna. *IOC Worksh Rep* 187:5–7
- Sahling H, Bohrmann G, Spiess V, Bialas J, Breitzke M, Ivanov M, Kasten S, Krastel S, Schneider R (2008) Pockmarks in the northern Congo Fan area, SW Africa: complex seafloor features shaped by fluid flow. *Mar Geol* 249:206–225
- Schmuck EA, Paull CK (1993) Evidence for gas accumulation associated with diapirism and gas hydrates at the head of the Cape Fear Slide. *Geo-Mar Lett* 13:145–152. doi:10.1007/BF01593187
- Shaw J, Courtney RC, Currie JR (1997) Marine geology of St. George's Bay, Newfoundland, as interpreted from multibeam bathymetry and back-scatter data. *Geo-Mar Lett* 17:188–194. doi:10.1007/s003670050025
- Somoza L, Hernández-Molina FJ, De Andres JR, Rey J (1997) Continental shelf architecture and sea-level cycles: Late Quaternary high-resolution stratigraphy of the Gulf of Cádiz, Spain. *Geo-Mar Lett* 17:133–139. doi:10.1007/s003670050018
- Somoza L, Díaz-del-Río V, Hernández-Molina FJ, León R, Lobato A, Alveirinho-Dias JM, Rodero J, TASYO Team (2000) New discovery of a mud-volcano field related to gas venting in the Gulf of Cadiz. Imagery of multibeam data and ultra-high resolution seismic. In: *Ext Abstr Vol 3rd Symp The Iberian Atlantic Margin*, 25–27 September 2000, Faro, pp 397–398
- Somoza L, Díaz-del-Río V, León R, Ivanov M, Fernández-Puga MC, Gardner JM, Hernández-Molina FJ, Pinheiro LM, Rodero J, Lobato A, Maestro A, Vázquez JT, Medialdea T, Fernández-Salas LM (2003) Seabed morphology and hydrocarbon seepage in the Gulf of Cádiz mud volcano area: acoustic imagery, multibeam and ultra-high resolution seismic data. *Mar Geol* 195:153–176
- Somoza L, Medialdea T, León R, Ercilla G, Vázquez JT, Farran M, Hernández-Molina FJ, González FJ, Juan C, Fernández-Puga MC (2012) Structure of mud volcano systems and pockmarks in the region of the Ceuta Contourite Depositional System (Western Alborán Sea). *Mar Geol* 332(334):4–26
- Stadnitskaia A, Ivanov M, Gardner J (2000) Hydrocarbon gas composition and distribution in surface sediments of mud volcanic province. Gulf of Cadiz. NE Atlantic. In: *Abstr Vol 6th Int Conf Gas in Marine Sediments*, 5–9 September 2000, St. Petersburg, pp 126–129
- Stadnitskaia A, Ivanov M, Blinova V, Kreulen R, Van Weering TCE (2006) Molecular and carbon isotopic variability of hydrocarbon gases from mud volcanoes in the Gulf of Cadiz, NE Atlantic. *Mar Petrol Geol* 23:281–296
- Stow D, Hernández-Molina FJ, Hodell D, Alvarez Zarikian CA (2011) Mediterranean outflow: environmental significance of the Mediterranean Outflow Water and its global implications. *IODP Sci Prosp* 339. doi:10.2204/iodp.sp.339.2011
- Talukder AR, Comas MC, Soto JI (2003) Pliocene to recent mud diapirism and related mud volcanoes in the Alborán Sea (Western Mediterranean). In: Maltman A, Van Rensbergen P, Morley C, Cartwright J (eds) Mobilisation of subsurface sediments. *Geol Soc Lond Spec Publ* 216:443–459
- Taylor MH, Dillon WP, Pecher IA (2000) Trapping and migration of methane associated with the gas hydrate stability zone at the Blake Ridge Diapir—new insights from seismic data. *Mar Geol* 164:79–89
- Vázquez JT, Vegas R (1996) Estructura profunda de la Cuenca del Mar de Alborán: margen continental nororiental y zona de transición hacia la Cuenca Surbalear. *Geogaceta* 20:962–965
- Vázquez A, Bruno M, Izquierdo A, Macías D, Ruiz-Cañavate A (2008) Meteorologically forced subinertial flows and internal wave generation at the main sill of the Strait of Gibraltar. *Deep-Sea Res* 55: 1277–1283
- Viana AR (2008) Economic relevance of contourites. In: Rebesco M, Camerlenghi A (eds) *Contourites, Developments in Sedimentology*, vol. 60. Elsevier, Amsterdam, pp 493–510
- Vogt PR, Gardner J, Crane K, Sundvor E, Bowles F, Cherkashev G (1999) Ground-truthing 11- to 12-kHz side-scan sonar imagery in the Norwegian–Greenland Sea: Part I: Pockmarks on the Vestnesa Ridge and Storegga slide margin. *Geo-Mar Lett* 19:97–110. doi:10.1007/s003670050098
- Wood WT, Gettrust J, Chapman NR, Spence GD, Hyndman RD (2002) Decreased stability of methane hydrates in marine sediments due to phase boundary roughness. *Nature* 420:656–660